Department of Orthodontics

CASE WESTERN RESERVE UNIVERSITY

SCHOOL OF DENTAL MEDICINE

GRADUATE STUDIES

We hereby approve the thesis of

Cynthia C. Leung

Candidate for the degree Master of Science

in Dentistry.

Signed: _____ DDS, MSD
(Chairperson)

_____

_____ L. PALOMO

_____

_____

Date: July 16, 2008

ACCURACY AND RELIABILITY OF CONE BEAM COMPUTED TOMOGRAPHY FOR MEASUREMENT OF ALVEOLAR BONE HEIGHT AND DETECTION OF BONY DEHISCENCES AND FENESTRATIONS

by

CYNTHIA C. LEUNG

Submitted in partial fulfillment of the requirements for

the degree of Master of Science in Dentistry

Thesis Advisors: Richard Griffith, D.D.S., M.S.D.

Mark G. Hans, D.D.S., M.S.D.

Department of Orthodontics

School of Dental Medicine

CASE WESTERN RESERVE UNIVERSITY

July 17, 2008

ACCURACY AND RELIABILITY OF CONE BEAM COMPUTED TOMOGRAPHY FOR MEASUREMENT OF ALVEOLAR BONE HEIGHT AND DETECTION OF BONY DEHISCENCES AND FENESTRATIONS

Abstract

by

CYNTHIA C. LEUNG

Introduction: To determine the accuracy and reliability of low milliamperage (2 mA), large voxel (0.38 mm), CBCT images for measurement of alveolar bone height and detection of naturally occurring buccal bony dehiscences and fenestrations. **Materials and Methods:** Thirteen dry human skulls with 334 teeth were scanned on a Hitachi CB MercuRay™ CT using the largest FOV and lowest ma settings. Measurements were performed on each tooth in the volume rendering mode from the cusp/incisal tip to the cementoenamel junction (CEJ) and from the cusp/incisal tip to the bone margin along the long axis of the tooth. Each tooth was also examined for the presence of dehiscence or fenestration. The dehiscences

and fenestrations were further verified by examining the corresponding cross-sectional slice data. Before the final analysis, measurements were adjusted for a known systematic error by adding the size of one voxel (0.38 mm) to each measure. Accuracy of CBCT measurements was determined by comparing the means, mean differences, absolute mean differences, and Pearson's correlation coefficient with those of direct measurements. Accuracy for detection of defects was determined using sensitivity and specificity. The positive and negative predictive values were also calculated. The intraclass correlation coefficient was used to assess reliability. **Results:** CBCT measurements showed mean deviations of 0.1±0.5 mm for measurements to the CEJ and 0.2±1.0 mm to the bone margin. The absolute value of the mean differences was 0.4±0.3 mm for the CEJ and 0.6±0.8 mm for the bone margin. The sensitivity and specificity of CBCT for fenestrations were both about 0.80 while the specificity for dehiscences was higher (0.95) and the sensitivity lower (0.40). As expected for defects with a low incidence, the negative predictive values were high (≥0.95) and the positive predictive values low

(dehiscence =0.50 and fenestration =0.25). The reliability of all measurements was high ($r \geq 0.94$). **Conclusions:** Using a voxel size of 0.38 mm at 2 mA, CBCT alveolar bone height can be measured to an accuracy of about 0.6 mm and root fenestrations can be identified with greater accuracy than dehiscences.

DEDICATION

This thesis is dedicated to:

My late mom and dad, without whom I would not have been in this world, for all the sacrifices you made and for giving me the opportunities that you never had yourselves. You will always be in my heart.

To all my sisters - Sis, Cathy, Chunica, and Grace - I appreciate your continual support and love throughout all these years.

My husband, Daniel Ng, without whom I would never have gotten this far: I am lucky to have you in my life. I appreciate your unconditional love, immense understanding, and unwavering support. Thank you for helping me pursue my dreams, for helping me through the tough times, and for keeping me on track. I love you more than I can ever express.

ACKNOWLEDGEMENTS

Thank you, Dr. Mark Hans for accepting me into the Department of Orthodontics at Case Western Reserve University, one of the finest orthodontic programs in the country. I have felt really lucky from day one and I am sure I will continue to feel the same in the future. You have truly made the program unique and special with your extraordinary vision, dedication, and passion toward educating orthodontic residents, not only your own, but residents all over the world. Thank you for all the mentorship during the past two years, which have helped me grow personally and professionally. Most importantly, thank you for guiding me through my thesis project.

Thank you, Dr. Richard Griffith for being my thesis advisor. I appreciate your guidance, patience, and understanding. Thank you for reading through all my drafts and providing helpful input.

Thank you, Dr. Leena Palomo for becoming a member of my thesis committee. I appreciate all your advice and

input which helped made my thesis as complete as possible. I also appreciate your friendship and encouragement.

Thank you, Dr. Martin Palomo for sharing your vast technical and clinical expertise with CBCT imaging.

Thank you, Cynthia McCaughey for all your help with the CBCT imagings during my data collection.

Thank you, Mrs. LaVerne Vogel for keeping the department running smoothly and for helping me schedule and reschedule my committee meetings and providing important administrative help.

Thank you, Dr. Sebastian Baumgaertel for being a great "big brother" during my first year and for staying around as an instructor. You have great principles and you will be a great clinician as well as a great educator.

Thank you to the Class of 2007. Thank you, Drs. Jeffrery Kwong and Alika Crew for your friendship and support.

Thank you to the Platinum Boys, the Class of 2008. Thank you, Dr. Austin Phoenix for being a wonderful "big brother". I appreciated your help when I was running behind with patients. Thank you, Dr. Boyd Martin III for

being a great friend and teacher. I learned a lot from you, not only academically, but also on a personal level. Thank you, Dr. John Ballrick for helping me with clinical questions and for taking the time to explain everything.

Thank you to my class. Thank you, Dr. Wanvadee Shewinvanakitkul for being my buddy at the Triangle. I enjoyed going to movies and shows with you as well as dinners and conversations at Siam Café and Richie's over the past couple of years. Thank you, Dr. Breyn Peters-Schuster for being who you are. I admire your candor and your wit. Thank you, Dr. Kurt Kacer for keeping me company at the clinic at nights. You made it easier to pass the time.

Thank you, Dr. Xing-Zhong "John" Zhang for being my friend and offering your help when needed. You will be a very knowledgeable Chair with your Western and Eastern orthodontic and cultural cross-training.

Thank you, Dr. David Sullivan for being a wonderful "little brother" and for helping out when necessary.

Thank you to the rest of Class of 2010, Drs. Nikolaos Evangelinakis, Monica Velez, and Lisa Austin for your friendship. You are a fun group.

Thank you, Dr. Eleftheria Karamitsou, Class of 2011 for your friendship and assistance during the critical moments in clinic.

And lastly, but not the least, a special "thank you" to all the faculty members for dedicating your time to teaching us and sharing your wealth of experience and knowledge. I have learned a lot from each and every one of you.

TABLE OF CONTENTS

ABSTRACT ii

DEDICATION v

ACKNOWLEDGEMENTS vi

TABLE OF CONTENTS x

LIST OF FIGURES xi

LIST OF TABLES xii

LITERATURE REVIEW 1

STATEMENT OF HYPOTHESES 11

MANUSCRIPT 12

APPENDIX I: STATISTICS 47

APPENDIX II: RAW DATA 65

TABLE A: Abbreviations 66

TABLE B: Raw and adjusted data from CBCT (accuracy) 67

TABLE C: Raw data from Direct (accuracy) 76

TABLE D: Raw data from CBCT (reliability) 86

TABLE E: Raw data from Direct (reliability) 88

REFERENCES 90

LIST OF FIGURES

Figure Page

1. Positioning of skull for CBCT imaging 39

2. Illustration of 3D volume rendering and optimization 40

3. Illustration of measuring technique on CBCT 41

4. Detection of fenestrations 45

5. Evaluation of CBCT tcejcA measurements for normality. 48

6. Evaluation of CBCT tbmcA measurements for normality. 49

7. Evaluation of Direct TCEJD measurements for normality 50

8. Evaluation of Direct TBMD measurements for normality 51

LIST OF TABLES

Table Page

1. Description of variables 42

2. Distribution of teeth examined by tooth type 42

3. Measurement accuracy of T-CEJ and T-BM by means, mean differences, standard deviations, and correlations 43

4. Summary of Direct and CBCT results for the presence of dehiscence or fenestration by tooth type 43

5. Detection of fenestrations and dehiscences by CBCT versus Direct 44

6. Sensitivity and specificity of CBCT for detection of fenestrations and dehiscences 44

7a: Analysis of dehiscence artifacts by cortical bone thickness 45

7b: Analysis of fenestration artifacts by cortical bone thickness 45

8. Intra-operator reliability for T-CEJ and T-BM measurements by means, mean differences, standard deviations, and intraclass correlations 46

9. Intra-operator reliability for T-Fen1 and T-Fen2 measurements by means, mean differences, standard deviations, and intraclass correlations 46

10: Descriptive statistics for CBCT tcejcA measurements 48

11: Descriptive statistics for CBCT tbmcA measurements 49

12: Descriptive statistics for Direct TCEJD measurements ..... .50

13: Descriptive statistics for Direct TBMD measurements 51

14: Paired Samples Statistics for Direct and CBCT T-CEJ Measurements 52

15: Paired Samples Correlations for Direct and CBCT T-CEJ Measurements 52

16: Paired Samples Test for Direct and CBCT T-CEJ Measurements 52

17: Paired Samples Statistics for Direct and CBCT T-BM Measurements 53

18: Paired Samples Correlations for Direct and CBCT T-BM Measurements 53

19: Paired Samples Test for Direct and CBCT T- T-BM Measurements 53

20: Descriptive Statistics for Bone Thicknesses Measured on Slice Data on Excluded Dehiscences 54

21: Descriptive Statistics for Bone Thicknesses Measured on Slice Data on Excluded Fenestrations 54

22: dehcA (Adjusted) * DEHD Crosstabulation 55

23: dehc (unadjusted) * DEHD Crosstabulation 55

24: fencA (Adjusted) * DEHD Crosstabulation 56

25: fenc (unadjusted) * DEHD Crosstabulation 56

26: Descriptive Statistics for CBCT tcejc at Timepoint 1 and Timepoint 2 57

27: Intraclass Correlation Coefficient for CBCT tcejc at Timepoint 1 and Timepoint 2 57

28: Descriptive Statistics for CBCT tbmc at Timepoint 1 and Timepoint 2 58

29: Intraclass Correlation Coefficient for CBCT tbmc at Timepoint 1 and Timepoint 2 58

30: Descriptive Statistics for CBCT tfen1 at Timepoint 1 and Timepoint 2 59

31: Intraclass Correlation Coefficient for CBCT tfen1 at Timepoint 1 and Timepoint 2 59

32: Descriptive Statistics for CBCT tfen2 at Timepoint 1 and Timepoint 2 60

33: Intraclass Correlation Coefficient for CBCT tfen2 at Timepoint 1 and Timepoint 2 60

34: Intraclass Correlation Coefficient for Direct TCEJD at Timepoint 1 and Timepoint 2 61

35: Descriptive Statistics for Direct TCEJD at Timepoint 1 and Timepoint 2 61

36: Descriptive Statistics for Direct TBMD at Timepoint 1 and Timepoint 2 62

37: Intraclass Correlation Coefficient for Direct TBMD at Timepoint 1 and Timepoint 62

38: Descriptive Statistics for Direct TFEN1D at Timepoint 1 and Timepoint 2 63

39: Intraclass Correlation Coefficient for Direct TFEN1D at Timepoint 1 and Timepoint 63

40: Descriptive Statistics for Direct TFEN2D at Timepoint 1 and Timepoint 2 64

41: Intraclass Correlation Coefficient for Direct TFEN2D at Timepoint 1 and Timepoint 64

Literature Review

Despite many reports in the literature on the various uses of cone beam computed tomography (CBCT), studies on the accuracy and image quality of CBCT for assessing bone morphology have been limited. Of those reported, most have been done using the NewTom QR DVT 9000 (Quantitative Radiology, Verona, Italy), Accuitomo 3D (J. Morita Mfg Corp., Kyoto, Japan), or i-CAT (Xoran Technologies, Ann Arbor, MI, and Imaging Science International, Hatfield, PA) CBCT. Very few studies have been reported on the accuracy of the CB MercuRay (Hitachi Medical Corp, Kashiwa-shi, Chiba-ken, Japan). Most studies are based on phantom studies which are not accurate representations of anatomic structures or have compared CBCT to multislice spiral computed tomography (MSCT), multidetector-row helical computed tomography (MDCT), or spiral computed tomography (SCT) as gold standards, which are not without inaccuracies and have higher radiation and higher cost.

The first model of cone beam computed tomography that used a cone beam x-ray instead of the traditional fan beam was the dynamic spatial reconstructor (DSR) introduced by Ritman et. al in 1980. This was developed to image a volume instead of a slice as in conventional CT with "stop-action" pulsed radiation to minimize blurring effects from motion and high-temporal

resolution which were especially important for imaging of the heart, lungs, and circulation (Hoffman, et al, 1983, Ritman, et al, 1980). While the high-temporal resolution of DSR was useful in angiographic imaging with contrast agents, the volumetric anatomic structures generated were indistinct. (Iwasaki, et al, 1985). Additionally, the unit was not readily accessible, since it was expensive and weighed thirteen tons[2]. Over the past couple of decades, DSR has evolved into the current CBCT as less expensive x-ray tubes, along with more powerful personal computers and higher quality detectors allowed for relatively low radiation doses, and smaller size requirements for operation, making CBCT more affordable and feasible in smaller clinical office settings (Scarfe, et al, 2006)

The first CBCT commercially available in the United States in 2001 was the NewTom QR DVT 9000. Others soon followed. These included the CB MercuRay™, 3D Accuitomo, and i-CAT. Since then, CBCT has started to become more widely used and accepted in various disciplines of dentistry. It has been utilized in presurgical assessment of implant sites (Garg, 2007, Hatcher, et al, 2003, Sato, et al, 2004); detection of hard tissue pathology of the maxillomandibular region (Schulze, et al, 2006); preoperative assessment of impacted mandibular third molars in relation to the inferior alveolar nerve (Pawelzik, et al, 2002); evaluation of impacted maxillary canines (Liu, et al, 2008, Walker, et al, 2005); surgical procedures involving enucleation of cysts, extirpation of odontogenic tumors, and apicoectomy (Nakagawa, et al, 2002);

evaluation of temporomandibular joint morphology, disease (Hintze, et al, 2007, Honda, et al, 2004, Tsiklakis, et al, 2004) and treatment of temporomandibular joint disorders (Honda, et al, 2004, Honda, et al, 2006); evaluation of upper airway volume in adolescents and patients with obstructive sleep apnea (Aboudara, et al, 2003, Ogawa, et al, 2005); and diagnosis and treatment planning in orthodontics (Hatcher, et al, 2004, Maki, et al, 2003, Nakajima, et al, 2005) as well as three-dimensional superimpositions to assess growth and treatment changes (Cevidanes, et al, 2006, Cevidanes, et al, 2007).

Studies that examined the accuracy of CBCT included Marmulla et al. (Marmulla, et al, 2005) who focused on the geometric accuracy of the NewTom 9000 using a polymethylmethacrylate cube with 216 measuring points of known dimensions. They found the accuracy was 0.13 mm with a standard deviation of 0.09 mm without geometric deviations or other non linear distortions. While this study showed how accurate the image was when the object was an almost perfect geometric shape with uniformed density and absorption, this did not show how accurate it was for a subject that was not geometrically proportional and had varying radiodensity, such as the human head. Therefore, the study was not clinically relevant.

This issue was partially addressed by data from Loubele et al. (Loubele, et al, 2006) They compared images of anthropomorphic head phantoms and two patients each acquired on one of three different CBCT's

(NewTom 9000, 3D Accuitomo, i-CAT) and with a corresponding MSCT image as the gold standard to determine the accuracy of CBCT. The CBCT images were geometrically aligned with the corresponding MSCT image by automated image registration using a method of maximization of mutual information (MMI) where identical anatomic locations on the CBCT images could be transferred onto the MSCT images by means of a mathematical registration algorithm. The accuracy of CBCT was interpreted as the difference in bone thickness measured at identical anatomic locations on the CBCT and MSCT images. The accuracy was found to be varied for the three CBCTs and depended on the location of the measurements and whether the images were smoothed (voids filled) or un-smoothed. The NewTom 9000 had larger measurements than the MSCT while the 3D Accuitomo images and i-CAT images were smaller. The measurements varied from +0.73+/-0.62 mm for the NewTom 9000 to -1.19+/-1.00 mm for the 3D Accuitomo. Although this study demonstrated that there were statistically significant differences in the measurements, they were deemed clinically insignificant since most of the differences were at a sub-millimeter level. However, the results were based on a single image acquired on each CBCT machine and a corresponding MSCT with no physical measurements available for comparison to determine which imaging modality was closer to the anatomic truth. The lack of sufficient sample size and true gold standard decreased the validity of the results. Moreover, the MSCT machines used were all different,

making it hard to compare the results. The magnification may be different for all three CBCTs simply because different MSCT machines were used. No standardization of the MSCT machines was performed in this pilot study. Additionally, the error associated with the method of MMI was not accessed between the CBCT and MSCT images. The error has been reported to vary from a subvoxel level for CT to MR (magnetic resonance) images up to as high as 1.97 mm for PET (positron emission tomography) to MR images (Maes, et al, 1997).

Kobayashi et al. (Kobayashi, et al, 2004) used cadaver mandibles as the anatomic truth to examine the accuracy of bone height measurements on CBCT and SCT. Five cadaver mandibles, with 2 mm reference holes made with a dental bur at seven locations on each mandible, were imaged with a SCT and a 3D Accuitomo limited cone beam computed tomography (LCBCT). The mandibles were then histologically sliced along the reference holes such that the planes of the slices corresponded to those of the reconstructed slices on the LCBCT and SCT images. Measurements were made from the superior border of the reference holes to the alveolar ridge on the same plane on the two different images and compared to measurements performed with a caliper on the physical specimen. The results showed a statistically significant difference between the two methods. The mean measurement error for the LCBCT was reported at 1.4%, ranging 0.1% to 5.2% (0.01 to 0.65 mm) while it was 2.2% for the SCT ranging 0% to 6.9% (0 to 1.11 mm).

The results showed that the CBCT images were more accurate than those of SCT. The reason for the higher accuracy was attributed to the nearly uniform spatial resolution in all directions for CBCT images whereas some spatial resolution was lost in the cross-sectional reformatting of SCT images.

Contrasting the results of the Loubele et al. study where the measurements were larger for the NewTom 9000 CBCT than the gold standard, the MSCT, Lascala et al (Lascala, et al, 2004) found the reverse was true, though physical measurement was used as the gold standard. Eight dry skulls were marked at 19 anatomical sites with 2 mm metal spheres and imaged using the CBCT. Measurements were performed on the landmarks on the CBCT images and directly on the physical skulls. In this case, real measurements were found to be consistently larger than those made from the CBCT images, although they were only statistically significant for measurements made at the internal cranial base. However, given the size of the metal markers, the authors did not specify how the tomographic images and the physical measurements were measured since it would make a difference whether both were measured at the periphery or the center of the markers. Another weakness was that no intraoperator reliability test was performed.

Another study to examine the accuracy of linear measurements on CBCT was by Hilger et al. (Hilgers, et al, 2005) Twenty-five human skulls, some with defects on the medial and lateral aspects of the

temporomandibular joints (TMJ), were imaged using the i-CAT CBCT and digital cephalograms made in three orthogonal planes (lateral cephalometric, posteroanterior, and submentovertex). Ten linear measurements were made from eleven predefined landmarks on the CBCT images in the 2D MPR (multiplanar reformatted) projections and cephalograms and compared to physical measurements made with a caliper. They found the measurements on the CBCT to be accurate with no significant difference from the anatomic truth whereas three of the five lateral cephalograms, four of the five posteroanteriors, and four of the six submental vertex cephalograms produced significantly greater measurements than the anatomic truth. They attributed the higher accuracy of CBCT to the inherent higher contrast of the 2D plane without anatomic noise from superimposition making it easier to identify landmarks. The study was well designed with fifty measurements for each variable with measurements repeated multiple times and a test of reliability was performed. However, one weakness of the study is that they reported the examiner was unblinded but self-controlled, but did not state how he was controlled. There was no mention of how operator bias was excluded. (One method, for example, would have been to have a lag period between measurements.) Additionally, distortions in other areas were not assessed, since measurements mainly involved the TMJ region.

The number of studies that examined the accuracy of CBCT at visualizing other structures such as alveolar bone dehiscences and

fenestrations have been few. This was addressed in a recent study by Pinsky et al. (Pinsky, et al, 2006) where the accuracy of CBCT for three-dimensional measurements of bony defects was evaluated. A human mandible specimen with simulated bone defects of various sizes and an acrylic block with machined cavitations were scanned using the i-CAT CBCT. As part of the study, five examiners were asked to measure the defects on the scanned images. The authors found that measurements made by the five examiners were more accurate on the acrylic block, with a mean deviation of less than 0.1 mm, than the mandible, with a mean deviation of less than 0.3 mm. The difference was statistically significant and the difference was attributed to the relative difficulty of defining the border of the defects with the presence of trabecular bone in the mandible. However, the error was within one or two voxels (0.2 mm/voxel) and the error was declared clinically acceptable. One weakness of the study was that the cavitations were created by machine and the bony defects were simulated making the boundaries more defined than natural defects. The accuracy may not be as closely correlated with real bony defects.

Another study to examine bony defects was by Mengel et al. (Mengel, et al, 2005). Periodontal defects including fourteen dehiscences (fixed at 12 mm high and 3 mm wide) and fenestrations (fixed at 4 mm high and 4 mm wide) were created in six pig and seven human mandibles. A clear reference surface was made by grinding the occlusal plane and gutta percha points

were positioned below the defects to aid in the measurement of the defects. The mandibles were imaged using various imaging systems including a 3D Accuitomo CBCT, CT, panoramic radiograph (PR), and intraoral radiograph (IR). Each defect along with the tooth was subsequently histologically sectioned and stained. Physical measurements made on these sections were used as the gold standard. The results showed that while dehiscences could not be assessed on the IR or PR images, they could be measured on the CT and CBCT images. The height and width of fenestrations were also measurable on the CT and CBCT images, but not in the IR and PR images. The third plane, depth, was measurable on CT and CBCT as well. The mean measurements for the four different methods showed the CT and CBCT had the most accurate measurements with a mean deviation from histological sections of 0.16+/-0.10 mm for CT and 0.19+/-0.11 mm for CBCT images. Pearson's correlation of the measurements showed a high correlation between the histological measurements and CT and CBCT images. However, one weakness of this study was that defects were, again, artificially created, making the borders of the defects more distinct in the images whereas natural defects may not have as clear borders and are therefore not as clearly visualized. Additionally, the manipulation of the mandibles with grinding of the occlusal plane to create a clear reference surface and placement of gutta percha for delineation of the defects also made it easier to

perform the measurements and reduced the measurement error, which contributed to overestimating the accuracy of the different imaging methods.

Since most studies examining the accuracy of CBCT for detecting bony defects have been performed on artificially created defects, the current study evaluated the accuracy and reliability of cone beam computed tomography (CBCT) for measuring the alveolar bone height and for the detection of naturally occurring dehiscences and fenestrations on human skulls. The information is clinically relevant since the use of CBCT in orthodontics and periodontics as well other dental disciplines for diagnosis and treatment planning will only continue to rise.

STATEMENT OF HYPOTHESES

There is no difference in the linear measurements of alveolar bone heights using cone beam computed tomography compared to physical measurements. If rejected, there would be a difference in the measurements between CBCT and physical measurements.

A second hypothesis is that there is no difference in the detection of dehiscences and fenestrations using cone beam computed tomography compared to direct assessment of physical dry human skulls. If rejected, there would be a difference in the detection of dehiscences and fenestrations between the CBCT machine and direct assessment.

ACCURACY AND RELIABILITY OF CONE BEAM COMPUTED TOMOGRAPHY FOR MEASUREMENT OF ALVEOLAR BONE HEIGHT AND DETECTION OF BONY DEHISCENCES AND FENESTRATIONS

Authors: Cynthia C. Leung, D.D.S.[a]

Richard Griffith, D.D.S., M.S.D.[b]

Leena Palomo, D.D.S., M.S.D.[c]

Mark G. Hans, D.D.S., M.S.D.[d]

a- Resident, Department of Orthodontics, Case Western Reserve University School of Dental Medicine, Cleveland, Ohio

b- Assistant Professor, Department of Orthodontics, Case Western Reserve University School of Dental Medicine, Cleveland, Ohio

c- Assistant Professor, Department of Periodontics, Case Western Reserve University School of Dental Medicine, Cleveland, Ohio

d- Professor and Chairman, Department of Orthodontics, Case Western Reserve University School of Dental Medicine, Cleveland, Ohio

Corresponding author:

Mark G. Hans, D.D.S., M.S.D.
Case Western Reserve University
School of Dental Medicine
Department of Orthodontics
10900 Euclid Ave.
Cleveland, OH 44106

ABSTRACT:

Introduction: To determine the accuracy and reliability of low milliamperage (2 mA), large voxel (0.38 mm), CBCT images for measurement of alveolar bone height and detection of naturally occurring buccal bony dehiscences and fenestrations.

Materials and Methods: Thirteen dry human skulls with 334 teeth were scanned on a Hitachi CB MercuRay^{TM} CT using the largest FOV and lowest ma settings. Measurements were performed on each tooth in the volume rendering mode from the cusp/incisal tip to the cementoenamel junction (CEJ) and from the cusp/incisal tip to the bone margin along the long axis of the tooth. Each tooth was also examined for the presence of dehiscence or fenestration. The dehiscences and fenestrations were further verified by examining the corresponding cross-sectional slice data. Before the final analysis, measurements were adjusted for a known systematic error by adding the size of one voxel (0.38 mm) to each measure. Accuracy of CBCT measurements was determined by comparing the means, mean differences, absolute mean differences, and Pearson's correlation coefficient with those of direct measurements. Accuracy for detection of defects was determined using sensitivity and specificity. The positive and negative predictive values were also calculated. The intraclass correlation coefficient was used to assess reliability

Results: CBCT measurements showed mean deviations of 0.1±0.5 mm for measurements to the CEJ and 0.2±1.0 mm to the bone margin. The absolute value of the mean differences was 0.4±0.3 mm for the CEJ and 0.6±0.8 mm for the bone margin. The sensitivity and specificity of CBCT for fenestrations were both about 0.80 while the specificity for dehiscences was higher (0.95) and the sensitivity lower (0.40). As expected for defects with a low incidence, the negative predictive values were high ($\geq$ 0.95) and the positive predictive values low (dehiscence = 0.50 and fenestration = 0.25). The reliability of all measurements was high ($r \geq 0.94$).

Conclusions: Using a voxel size of 0.38 mm at 2 mA, CBCT alveolar bone height can be measured to an accuracy of about 0.6 mm and root fenestrations can be identified with greater accuracy than dehiscences.

INTRODUCTION

Despite many reports in the literature on the various uses of cone beam computed tomography (CBCT), studies on the accuracy and image quality of CBCT for assessing bone morphology have been limited. Of those reported, most have been done using the NewTom QR DVT 9000 (Quantitative Radiology, Verona, Italy), Accuitomo 3D (J. Morita Mfg Corp., Kyoto, Japan), or i-CAT (Xoran Technologies, Ann Arbor, MI, and Imaging Science International, Hatfield, PA) CBCT. There have been a number of studies that have tested the measurement accuracy of the CB MercuRay. However, no studies have assessed the use of CBCT to study alveolar bone morphology in vivo. (Hitachi Medical Corp, Kashiwa-shi, Chiba-ken, Japan). Most studies have used radiographic phantoms[1,2] which do not accurately represent some anatomic structures like the tooth sockets and alveolar bone margins. Other studies have used human skulls but the defects measured were created by the operator[3-6]. Still other studies have compared CBCT to multislice spiral computed tomography (MSCT), multidetector-row helical computed tomography (MDCT), or spiral computed tomography (SCT)[1,7] as gold standards. The problem with comparing CBCT to other CT machines is that all CT's have some measurement error[8-10]. In addition, MSCT, MDCT and SCT use more radiation and have a higher cost making those machines of limited use for dentistry[11-13].

The first model of cone beam computed tomography that used a cone beam x-ray instead of the traditional fan beam was the dynamic spatial reconstructor (DSR) introduced by Ritman et al. in 1980. This was developed to image a volume instead

Department of Orthodontics

of a slice as in conventional CT with "stop-action" pulsed radiation to minimize blurring effects from motion and high-temporal resolution which were especially important for imaging of the heart, lungs, and circulation[14,15]. While the high-temporal resolution of DSR was useful in angiographic imaging with contrast agents, the volumetric anatomic structures generated were indistinct[16]. Additionally, the unit was not readily accessible, since it was expensive and weighed thirteen tons[2]. Over the past few decades, DSR has evolved into the current CBCT using less expensive x-ray tubes, along with more powerful personal computers and higher quality detectors, allowing for relatively low radiation doses, and smaller size requirements for operation, making CBCT more affordable and feasible in smaller clinical office settings[17].

According to the definition given by Carranza[18], fenestrations are defined as isolated areas in which the root is denuded of bone and the root surface is covered only by periosteum and overlying gingiva. Dehiscences are defined as bony defects in which the denuded areas involve the alveolar bone margin. The presence of these buccal alveolar bone defects decreases the bony support for the teeth. It is well documented that under certain conditions (i.e. presence of plaque-induced inflammation) a lack of bony support during orthodontic movement can be detrimental to the health of the tooth and the periodontium[19-21]. In addition, it is possible that orthodontic tooth movement could create alveolar bone defects[22-28]. Until recently, bony dehiscences and fenestrations could not be visualized by traditional two-dimensional radiography due to superimposition of contralateral

cortical bony or dental structures[29,30]. The development of computed tomography (CT) and especially cone beam computed tomography (CBCT) has provided a means to visualize these defects three-dimensionally[3,31]. The literature has reported the accuracy of computed tomography and cone beam computed tomography for measuring and identifying artificially created alveolar bone defects[3,4,6]. However, no studies have evaluated the use of CBCT to diagnose naturally occurring bony dehiscences and fenestrations in human skulls. In addition, no studies have determined the positive and negative predictive values when CBCT is used to diagnose alveolar bone defects. The purpose of this study was to evaluate the accuracy and reliability of three-dimensional cone beam computed tomography (CBCT) in the diagnosis of naturally occurring fenestrations and bony dehiscences.

In addition, this study evaluated the accuracy and reliability of three-dimensional cone beam computed tomography (CBCT) to measure the alveolar bone margins on dentate skulls. This is important because the identification of these alveolar bone defects prior to orthodontic treatment is helpful for the clinician when treatment planning. An undiagnosed buccal alveolar bone defect could occur in a small percentage of patients which could lead to greater potential for treatment relapse[32,33] or gingival recession resulting in an unaesthetic finish at the end of orthodontic treatment[34-37]. The first hypothesis is that there is no difference in the measurement of alveolar bone height using CBCT compared to physical measurements. The second hypothesis is that there is no difference in the detection of

dehiscences and fenestrations using the CBCT imaging system compared to direct assessment of physical dry human skulls.

MATERIALS AND METHODS

Dry human skulls were selected from the Hamann-Todd Skull Collection, at the Bolton-Brush Growth Study and the Museum of Natural History, Cleveland, OH. A preliminary screening of thirty-nine skulls consisting of 1040 teeth showed that the prevalence of dehiscences and fenestrations were approximately 11% and 8% of the teeth examined, respectively. These percentages were equivalent to the average of the rates reported in the literature[38-43]. A sample size estimation for a descriptive study using proportions was determined to be 240 at a confidence level of 99% and a confidence interval of 1% [44]. In addition, the sample size calculation for comparison of two groups using a standardized effective size of 0.25 mm based on previous studies at a 5% level of significance and an 80% power was found to be a minimum of 240. A sample of thirteen skulls with 334 teeth was selected with the following inclusion criteria: 1) between ages 18-35, 2) intact skulls with maxilla and mandible, 3) minimum of ten teeth per jaw, 4) lack of obvious pathology (cyst or tumor in the alveolar process) 5) no mechanical damage (chips, cracks, breaks in the alveolar process).

Skulls were scanned using a commercially available CBCT scanner (CB MercuRay™ Volumetric Digital Imaging Unit, Hitachi Medical Systems American, Inc., Twinsburg, OH). After assuring the calibration of the machine, the skulls were positioned in the center of the scanning table in the same orientation as a live patient

using vertical and horizontal light guides (Figure 1). To allow visualization of both maxillary and mandibular cusps, the maxillary and mandibular dentitions were discluded with a cotton roll at the anterior region. The scanning parameters used for imaging were 110 kVp, 2 mA, 9.6 sec/revolution, and a 12 inch field of view (P-mode). These settings produced a voxel size of 0.38 mm[45]. The settings used were the same as those used for orthodontic diagnosis and treatment planning in the graduate orthodontic clinic at Case Western Reserve University.

Raw data were collected and reconstructed into three-dimensional volumes using software provided by the manufacturer. The reconstructed data were exported and saved as Digital Imaging and Communications in Medicine (DICOM) files. The 512 two-dimensional slices were imported into a commercially available software program (Accurex^{TM} version 1.1 Cybermed Inc., Seoul, Korea) on a networked computer workstation (Dell, Windows NT) for secondary 3D reconstruction. The 3D volume rendering (VR) mode was utilized to display the CBCT images for evaluation and analysis. The radiodensity in Hounsfield units (HU) was adjusted by the operator to the threshold deemed optimal for visualization of the buccal alveolar bone (Figure 2). Based on a preliminary skull study the threshold window was fixed for all skulls at -280 HU and -510 HU at the upper and lower limits, respectively.

Figure 3 illustrates the measuring technique used for the CBCT images. All measurements were performed by the same operator (C.C.L.). Because of the tendency for fenestrations and dehiscences to occur on the labial/buccal surfaces[42,46] all measurements on the CBCT images were performed on the buccal surface parallel

to the long axis of the tooth. The first reference point was the cusp tip (T) for posterior dentition and the mid-incisal tip (T) for anterior dentition. The second reference point was the cementoenamel junction (CEJ) for the first measurement, the alveolar bone margin (BM) for the second measurement, and if a fenestration was present the coronal border of the fenestration for the third measurement (denoted as T-Fen1) and the apical border for the fourth measurement (denoted as T-Fen2). Since each molar has at least two buccal cusps, the mesiobuccal and the distobuccal cusps were both measured individually. Table 1 describes the variables used. Previous studies had used varying criteria for the identification of a dehiscence ranging from any defect greater than 1 mm that commenced close to the cementoenamel junction[41], to 4 mm apical to the interproximal bone crest[39,40,43], to exposure of half the root[38,42]. For the purposes of this study, to distinguish a dehiscence from horizontal bone loss due to periodontal disease, a dehiscence was defined as present when there was a "V" shaped defect along the bone margin and the distance between the CEJ and the alveolar bone height was 3 mm or greater. If a fenestration or dehiscence was found on the 3D volumetric view, it was further analyzed using the 2D slice data to verify the presence or absence of bone covering the root surface. Defects were recorded if no bone could be seen covering the root surface when examining the axial and coronal slices at the heights indicated by T-BM for dehiscences and between T-Fen1 and T-Fen2 for fenestrations.

The same measurements were performed directly on the physical skulls using a digital caliper calibrated to the nearest 0.01 mm (Code No.: 500-171-20 Model No.:

CD-6"CX Digimatic Caliper™, Mitutoyo American Corp, Plymouth, MI). To limit experimental bias, all measurements on the physical skulls were done at least 2 weeks after the CBCT measurements. Table 2 shows the distribution of the teeth examined by tooth type. One hundred sixty-seven teeth were examined in both the maxilla and mandible giving a total of 334 teeth. A total of 446 measurements were made since two reference points (mesial and distal cusps) were measured on the molars teeth.

Statistical Analysis

All statistical analyses were performed using the computer software Statistical Package for Social Sciences, SPSS™ 16.0 (SPSS Inc. Chicago, Il). All linear measurements were adjusted for a known systematic software measurement error that underestimated the distance between two points by one-half of a voxel at each endpoint. Therefore, 0.38 mm was added to each measurement to correct for this software error. For a complete discussion of this systematic error see Baumgaertel et al.[47]. Measurement accuracy was evaluated by comparing the means, mean differences, and absolute mean differences for linear measures. Two-tailed paired t-tests were used to examine differences between means and Pearson correlation coefficients were used to estimate the relationship between the direct (digital caliper) and indirect (CBCT) methods. A probability (P) value of ≤ 0.05 was used to assign statistical significance. Categorical data (presence or absence of fenestrations and dehiscences) were analyzed using 2x2 tables and the sensitivity, specificity, and positive and negative predictive values were calculated for both direct and indirect (CBCT) methods. The direct method was used as the gold standard for comparison.

Reliability

To determine the reliability of the methods, 65 randomly selected teeth (91 sites) were re-examined and re-measured using both methods at least two weeks after the initial measurements. The intra-operator reliability was assessed by calculating the intraclass correlation coefficient between measurements collected at timepoint 1 and timepoint 2.

RESULTS

Accuracy

The linear measurement accuracy of CBCT was demonstrated by the means, mean differences, and absolute mean differences between each pair of direct and CBCT measurements. Pearson correlation coefficients were also calculated for each pair of direct and indirect measurements. Table 3 shows these descriptive statistics for measurements from the tip to the cementoenamel junction (T-CEJ) and from the tip to the bone margin (T-BM) for all sites examined. The means for both CBCT and direct T-CEJ measurements were approximately equal (8.3 ± 1.4 mm vs. 8.3 ± 1.5 mm) while the mean differences between the two methods showed that the CBCT measurements were essentially equal to the direct measurements (-0.1 ± 0.5 mm). The absolute mean differences showed a difference of 0.4 ± 0.3 mm between the CBCT and direct measurements which was about the size of a voxel. The linear measurement from the cusp tip to bone margin (T-BM) was 0.2 ± 1.0 mm smaller on average for CBCT while the absolute mean differences were 0.6 ± 0.8 mm. Paired t-test statistics showed a significant difference between CBCT and direct measurements

to both CEJ and BM ($P \leq 0.01$). The correlation between CBCT and direct methods for T-CEJ measurements was high ($r=0.94$) as was the correlation for T-BM at 0.87.

The number of fenestrations detected by CBCT was more than three times higher than for direct examination (104 fenestrations by CBCT versus 32 by direct, see Table 4). The number of dehiscences was less for CBCT than for direct (43 dehiscences versus 52). Fenestrations were detected more often in the maxilla than in the mandible for both CBCT and direct whereas dehiscences were detected more often in the mandible than in the maxilla.

The CBCT and direct results were analyzed using 2x2 contingency tables (Table 5). For fenestrations, the sensitivity and specificity of CBCT were both at 0.81 (Table 6). For dehiscences, the specificity of CBCT was 0.95 whereas the sensitivity was 0.42. The negative predictive value for fenestrations, the probability that a negative test result (absence of fenestration) was truly negative, was 0.98, while the positive predictive value, the probability that a positive test result (presence of fenestration) was truly positive, was only 0.25. The negative predictive value for dehiscences was 0.93, while the positive predictive value was only 0.51. Sixteen false positive dehiscences were excluded by examining axial and coronal slices while two true positive dehiscences were eliminated. For fenestrations, 57 false positives were excluded when slice data were examined and no true positives were eliminated. The number of positives by CBCT and direct as well as the number of false positives by CBCT are illustrated in Figure 4.

Reliability

The intraclass correlation coefficients for the four continuous variables, T-CEJ, T-BM, T-Fen1, T-Fen2, showed excellent reliability for the direct (digital caliper) method with coefficients at 0.99 and the reliability for the CBCT method was rated as very good to excellent with coefficients ranging from 0.89 to 0.95 (Tables 8-9).

DISCUSSION

One aim of this study was to evaluate the accuracy and reliability of linear measurements of alveolar bone height using CBCT. To measure alveolar bone height requires identification of the alveolar bone margin and the cementoenamel junction. The accuracy of detection of these landmarks was measured independently. Interestingly, the identification of the CEJ was more accurate than the identification of the bone margin. This finding is understandable given the nature of CBCT images. The CEJ is the junction between enamel and cementum, two biological tissues of different densities. The accuracy of identifying this intersection is limited by the size of each voxel in the image. Therefore, the CEJ on the CBCT images used in this study should theoretically be able to be located within the margin of error of a single voxel, or about 0.38 mm. The actual margin of error was 0.4 mm. In contrast to the CEJ, the alveolar bone margin is the junction between cementum and bone, two tissues of similar density. Here the accuracy is limited not by voxel size but by the physical spatial resolution of the image. The physical spatial resolution of a CT image is determined by testing with a resolution phantom. For 2 mA, 12 inch CBCT

images on the Hitachi CB MercuRay, the physical resolution is 0.668 mm. The results of this study are consistent with this physical resolution limit since the bone margin was located with an accuracy of 0.6 mm. Both spiral CT and multislice CT have higher physical resolution so they might yield slightly better results, however, there is a ten fold increase in radiation with these other CT methods. Likewise, CBCT machines with lower mA settings might have higher margins for error in locating the bone margin. Ballrick et al.[53] demonstrated that the average image resolution for the clear separation of a series of four lines on CBCT (with a flat panel detector) was 0.622 mm for the 6 cm FOV and 0.860 mm for 13 cm FOV while Baba et al.[54] demonstrated that the resolution of the CBCT (with an image intensifier detector and charge coupled device) was about 0.6 mm for 25 cm FOV.

The loss in low contrast resolution as stated by Haaga et al.[56] may explain the inability to distinguish the interface or margin between two objects of similar densities such as the cementum on root surface and alveolar bone. The densities of cementum and bone are similar due to their similar hydroxyapatite content[18]. Cementum has 45% to 50% hydroxyapatite and bone has about 65%. Enamel, on the other hand has a hydroxyapatite content of about 97%, thus, resulting in a greater density difference between cementum and enamel than cementum and bone. Therefore, this density difference may explain why the cementum-enamel interfaces (cementoenamel junctions) were more accurately and reliably measured than at the cementum-bone interfaces (correlation coefficient of 0.94 versus 0.87). Additionally,

bone margins had a certain thickness that may have caused difficulty in selecting the point accurately for the measurement.

Using mandibles pre-drilled with reference holes, Kobayashi et al.[9] reported a mean measurement error (mean absolute difference) of 0.22 mm (± 0.15) to the bone margin between CBCT and direct measurements which was less than that found in the current study of 0.6 mm (± 0.8). As discussed in the previous paragraph, this difference is explained by the smaller voxel used in their study (0.125 mm) and the more well-defined reference points in the artificially created defects. Using a mean absolute measurement error, Mischkowski et al.[5] reported a similar accuracy of 0.26 mm (± 0.18 mm) on measurements also performed on fabricated holes at pre-defined distances on a dry skull. The voxel size used was 0.30 mm, but the accuracy may be overestimated compared to clinical settings due to the use of gutta percha points placed at the holes to improve visualization during measurements.

Of the previous studies performed to evaluate the accuracy of CBCT measurements, only a couple reported on the reliability of the method by repeating measurements on a small sample with a time interval between the first and second measures. Pinsky found the intraexaminer reliabililty by intraclass correlation coefficient (ICC) for CBCT ranged from 0.75 to 0.99. Baumgaertel et al.[47] found that the reliability of measuring variables relating to teeth on CBCT images was highly reliable with an intra-class correlation coefficient nearly 1.0. This study also showed a high reliability of both CBCT and direct methods with an intra-class correlation of 0.94 and 0.99, respectively. The slight decrease in reliability for CBCT

may be attributed to the difficulty in visualizing the CEJ or the bone margins as clearly as the crowns of the teeth.

A second aim was to evaluate the accuracy and reliability of CBCT for diagnosing naturally occurring buccal alveolar fenestrations and dehiscences on dry human skulls. Naturally occurring fenestrations and dehiscences were used because previously reported studies have used artificially created defects on phantoms or dry skulls where the detection of defects may be overestimated due to the distinct borders created by the operator. Mengel et al.[3] reported that all dehiscences and fenestrations in pig and dry human mandibles were identifiable on the CBCT; however these were artificially created and gutta percha points were used to aid visualization. Misch et al.[4] also reported that all periodontal defects, artificially created on a mandible, were identifiable and measurable. Similarly, Pinsky et al.[6] also were able to identify bony defects and cavitations on human mandibles and acrylic blocks, but, again, these were artificially created. Since naturally occurring defects have more gradual and tapering margins, they may not be visualized on CBCT as easily as those created by an operator. Therefore, these studies may not provide a true assessment of CBCT for diagnosing alveolar bone defects.

Indeed, the results from the current study showed that the indirect assessment of buccal alveolar bone defects overlying roots was not as accurate as previously reported. There was a much higher rate of false positives (false fenestrations) identified using CBCT; three times the number of fenestrations detected on CBCT compared to direct (physical skull examination). Along with false positives there

were also a significant number of false negatives where true defects were missed on CBCT. More than half of the dehiscences were not detected on CBCT (30 out of 52 dehiscences, data not shown)

Comparing to the study by Fuhrmann et al.[31] where a conventional CT (high resolution CT) was used to assess dehiscences and fenestrations artificially created on human skulls, the current study demonstrates a higher sensitivity of CBCT for fenestrations (80% versus 70% for CT), but a lower sensitivity for dehiscences (42% versus to 70% for CT). A larger proportion of true dehiscences were missed on CBCT compared to CT. This is likely due to the fact that the bone margin tapered to a thickness less than the physical limits of the CBCT and therefore the bone margin could only be identified within this 0.6 mm limit.

The spatial resolution limitations of the CBCT meant that areas where the bone was less than 0.6 mm thick were seen on the image as areas without bone present. The extent of bone thickness required to be depicted on CBCT was elucidated by the bone thicknesses of the false positive defects measured on axial and coronal slice data (see Tables 7a and 7b). The smallest thickness measured on axial and coronal sections was 0.6 mm suggesting that this was the minimum thickness required for bone to be measurable and distinguishable from the root surface. This required minimum bone thickness may partially explain the higher number of false positive fenestrations found in the maxilla, where the cortical bone is less dense than that of the mandible[55]. Another reason for the increased number of false positive fenestrations in the maxilla may be the higher prevalence of root prominence in the

maxilla. Root prominence influences the overlying alveolar bone thickness. The overlying bone tends to be thinner where the root is prominent [38,40,42]. Nevertheless, the study showed that there were two possibilities when bone was not visualized on CBCT: the bone may be truly missing or the bone thickness was less than 0.6 mm.

The ability to visualize two objects close together may also depend on the image quality. Image quality is influenced by the scanning parameters used. The effect of milliamperage on image quality had been studied extensively. Comparing CT images taken at different milliamperage settings ranging from 6 mA to 100 mA, Haaga et al.[56] found that there was a loss in low contrast resolution when the lower milliamperage settings were used (6 mA and 20 mA) whereas the resolution was the same at 40 mA and 100 mA. Palomo et al.[57] also found a difference in image resolution that was dependent on the milliamperage used. Using a C-phantom with an acrylic base and a series of metal lines in water and the method of Q-sort conducted on professionals experienced with radiographs, they showed that higher milliamperage with a copper filter demonstrated better image quality and higher spatial resolution. However, they suggested that for dental use a compromise between image quality and radiation dose needs to be considered based on the ALARA (As Low As Reasonably Achievable) principle.

Thus, the effect of different milliamperage settings may be a factor in the differences observed in the current study with those of previous studies. Misch et al.[4] and Pinsky et al.[6] used scanning parameters that were much higher than the clinically used parameters employed in the current study. Misch el al. used 47.7 mA, 120 kVp,

and 20 sec, while Pinsky et al. used 98 mA, 120 kVp, and 20 sec. Both of these studies demonstrated that all artificially created alveolar bone defects were identified and measurement accuracy was high. Similarly Mischkowski et al. used 28 mA compared to studies reporting a lower measurement accuracy, such as that of Hilger et al. where 1-3 mA was used and that of Lascala et al. where 7 mA was used. Studies that showed a lower accuracy or sensitivity as in the current study also used lower tube current. Honda et al.[52] used 2 mA, 80 kVp, and 17 sec, whereas Hintz et al.[51] used an even lower milliamperage of 0.5 mA, 110 kVp, and 5-7 sec.

Finally, the results still support the use of CBCT for detection of buccal bony defects such as dehiscences and fenestrations. The low positive predictive values for dehiscences and fenestrations are less critical since the prevalence of the defects are low at about or less than 10% as reported in most studies[38-40,42,43]. Due to the low prevalence, it becomes more important that true negatives be identified correctly to avoid unnecessary alarm. Thus, the high negative predictive values of 0.95 for dehiscences and 0.98 for fenestrations found in the current study provide evidence that when a defect is not detected on CBCT, most likely it is not there and gives some assurance that a buccal defect is mostly likely not present.

As with most studies, there were some limitations with the current study as well. First, the CBCT scanner employed in this study, was calibrated as a routine using a designated phantom with densities simulating a live person, however, the dried skulls used did not have any soft tissue. Soft tissues have attenuation coefficients which may affect the x-ray beam going through the skulls and hence the

final image. The final image is dependent on the algorithms used during the calibration process. Since the standard used for the calibration was for a live person, the calibration may not be optimal for the dried skulls. Calibration is an important step in primary reconstruction of scanned images to eliminate reconstruction inaccuracies and errors emanating from the imaging system. Without proper calibration, the images may have excessive artifacts. Thus, perhaps, the machine could have been calibrated with a more appropriate standard to sufficiently eliminate any imaging artifacts inherent in the imaging system. Additionally, due to the skulls being part of a museum collection, it was not possible to provide some resemblance of soft tissue such as using balloons filled with water as performed in the study by Hilger et al.[49]. Alternatively, cadaver heads with soft tissue could be used to better simulate a live person. However, a problem arising from this approach may be a limiting sample size and finding a sufficient number of defects for the study.

Another potential limitation of the current study is the possible operator error introduced by fixing the Hounsfield threshold window for all the skulls. The Hounsfield values for the upper and lower limits of the window were based on a histogram study of a single skull. However, due to the effect of thickness and radiodensity of the subject on the attenuation of radiation and the resulting image[59], the threshold used may not be optimal for all of the skulls. Each skull could have been optimized individually. One way to amend this problem may be to use an operator-independent and a less subjective method of classifying defects, such as utilizing the region of interest (ROI) tool and identifying bony defects based on

segmentation methods. The defect could be identified more objectively using the Hounsfield histogram for the segmented area. The difference between the bone surface and root may be more apparent by examining the Hounsfield values.

CONCLUSION

This study showed that measurements on CBCT were not as accurate as direct measures made on skulls. The differences found between the direct and CBCT methods were likely due to limitations in spatial resolution of the CBCT images. Location of the CEJ was found to be accurate to within 0.4 mm and location of the bone margin to within 0.6 mm. The correlation between CBCT and direct measurements was high for measurements to the CEJ ($r=0.94$) as well as to the bone margin ($r=0.87$). The reliability of the CBCT method was high, with an intraclass correlation coefficient of about 0.95.

The diagnostic value of CBCT for the detection of buccal defects was high for fenestrations where both sensitivity and specificity were about 0.80. For dehiscences, the specificity was high at 0.95, but the sensitivity was low at 0.40. The positive predictive value was 0.50 for dehiscences and 0.25 for fenestrations. In other words, when a defect was detected on CBCT, it was a true dehiscence about half of the time and a true fenestration about a quarter of the time. The negative predictive values, however, were high for both at 0.93 for dehiscences and 0.98 for fenestrations. This means when a defect is not detected on CBCT, most likely there is no defect.

REFERENCES

1. Loubele M, Maes F, Schutyser F, Marchal G, Jacobs R, Suetens P. Assessment of bone segmentation quality of cone-beam CT versus multislice spiral CT: a pilot study. Oral Surg Oral Med Oral Pathol Oral Radiol Endod. 2006 Aug;102(2):225-34.

2. Marmulla R, Wortche R, Muhling J, Hassfeld S. Geometric accuracy of the NewTom 9000 Cone Beam CT. Dentomaxillofac Radiol. 2005 Jan;34(1):28-31.

3. Mengel R, Candir M, Shiratori K, Flores-de-Jacoby L. Digital volume tomography in the diagnosis of periodontal defects: an in vitro study on native pig and human mandibles. J Periodontol. 2005 May;76(5):665-73.

4. Misch KA, Yi ES, Sarment DP. Accuracy of cone beam computed tomography for periodontal defect measurements. J Periodontol. 2006 Jul;77(7):1261-6.

5. Mischkowski RA, Pulsfort R, Ritter L, Neugebauer J, Brochhagen HG, Keeve E, Zoller JE. Geometric accuracy of a newly developed cone-beam device for maxillofacial imaging. Oral Surg Oral Med Oral Pathol Oral Radiol Endod. 2007 Oct;104(4):551-9.

6. Pinsky HM, Dyda S, Pinsky RW, Misch KA, Sarment DP. Accuracy of three-dimensional measurements using cone-beam CT. Dentomaxillofac Radiol. 2006 Nov;35(6):410-6.

7. Hashimoto K, Kawashima S, Araki M, Iwai K, Sawada K, Akiyama Y. Comparison of image performance between cone-beam computed tomography for dental use and four-row multidetector helical CT. J Oral Sci. 2006 Mar;48(1):27-34.

8. Hu H, He HD, Foley WD, Fox SH. Four multidetector-row helical CT: image quality and volume coverage speed. Radiology. 2000 Apr;215(1):55-62.

9. Kobayashi K, Shimoda S, Nakagawa Y, Yamamoto A. Accuracy in measurement of distance using limited cone-beam computerized tomography. Int J Oral Maxillofac Implants. 2004 Mar-Apr;19(2):228-31.

10. Karger CP, Hipp P, Henze M, Echner G, Hoss A, Schad L, Hartmann GH. Stereotactic imaging for radiotherapy: accuracy of CT, MRI, PET and SPECT. Phys Med Biol. 2003 Jan 21;48(2):211-21.

11. Lecomber AR, Yoneyama Y, Lovelock DJ, Hosoi T, Adams AM. Comparison of patient dose from imaging protocols for dental implant planning using conventional radiography and computed tomography. Dentomaxillofac Radiol. 2001 Sep;30(5):255-9.

12. Mah JK, Danforth RA, Bumann A, Hatcher D. Radiation absorbed in maxillofacial imaging with a new dental computed tomography device. Oral Surg Oral Med Oral Pathol Oral Radiol Endod. 2003 Oct;96(4):508-13.

13. Scaf G, Lurie AG, Mosier KM, Kantor ML, Ramsby GR, Freedman ML. Dosimetry and cost of imaging osseointegrated implants with film-based and computed tomography. Oral Surg Oral Med Oral Pathol Oral Radiol Endod. 1997 Jan;83(1):41-8.

14. Hoffman EA, Sinak LJ, Robb RA, Ritman EL. Noninvasive quantitative imaging of shape and volume of lungs. J Appl Physiol. 1983 May;54(5):1414-21.

15. Ritman EL, Kinsey JH, Robb RA, Gilbert BK, Harris LD, Wood EH. Three-dimensional imaging of heart, lungs, and circulation. Science. 1980 Oct 17;210(4467):273-80.

16. Iwasaki T, Ritman EL, Fiksen-Olsen MJ, Romero JC, Knox FG. Renal cortical perfusion--preliminary experience with the dynamic spatial reconstructor (DSR). Ann Biomed Eng. 1985;13(3-4):259-71.

17. Scarfe WC, Farman AG, Sukovic P. Clinical applications of cone-beam computed tomography in dental practice. J Can Dent Assoc. 2006 Feb;72(1):75-80.

18. Carranza F, Newman M, Takei H. The Tooth-Supporting Structures. Clinical Periodontology. 9 ed. Philadephia W.B. Saunders; 2002.

19. Ericsson I, Thilander B, Lindhe J, Okamoto H. The effect of orthodontic tilting movements on the periodontal tissues of infected and non-infected dentitions in dogs. J Clin Periodontol. 1977 Nov;4(4):278-93.

20. Wennstrom JL, Stokland BL, Nyman S, Thilander B. Periodontal tissue response to orthodontic movement of teeth with infrabony pockets. Am J Orthod Dentofacial Orthop. 1993 Apr;103(4):313-9.

21. Artun J, Urbye KS. The effect of orthodontic treatment on periodontal bone support in patients with advanced loss of marginal periodontium. Am J Orthod Dentofacial Orthop. 1988 Feb;93(2):143-8.

22. Zachrisson BU, Alnaes L. Periodontal Condition in Orthodontically Treated and Untreated Individuals I. Loss of Attachment, Gingival Pocket Depth and Clinical Crown Height. Angle Orthod. 1974;43(4):402-11.

23. Wehrbein H, Bauer W, Diedrich P. Mandibular incisors, alveolar bone, and symphysis after orthodontic treatment. A retrospective study. Am J Orthod Dentofacial Orthop. 1996 Sep;110(3):239-46.

24. Karring T, Nyman S, Thilander B, Magnusson I. Bone regeneration in orthodontically produced alveolar bone dehiscences. J Periodontal Res. 1982 May;17(3):309-15.

25. Wainwright WM. Faciolingual tooth movement: its influence on the root and cortical plate. Am J Orthod. 1973 Sep;64(3):278-302.

26. Garib DG, Henriques JF, Janson G, de Freitas MR, Fernandes AY. Periodontal effects of rapid maxillary expansion with tooth-tissue-borne and tooth-borne expanders: a computed tomography evaluation. Am J Orthod Dentofacial Orthop. 2006 Jun;129(6):749-58.

27. Zachrisson BU, Alnaes L. Periodontal condition in orthodontically treated and untreated individuals. II. Alveolar bone loss: radiographic findings. Angle Orthod. 1974 Jan;44(1):48-55.

28. Sarikaya S, Haydar B, Ciger S, Ariyurek M. Changes in alveolar bone thickness due to retraction of anterior teeth. Am J Orthod Dentofacial Orthop. 2002 Jul;122(1):15-26.

29. Lang NP, Hill RW. Radiographs in periodontics. J Clin Periodontol. 1977 Feb;4(1):16-28.

30. Rees TD, Biggs NL, Collings CK. Radiographic interpretation of periodontal osseous lesions. Oral Surg Oral Med Oral Pathol. 1971 Jul;32(1):141-53.

31. Fuhrmann R. Three-dimensional interpretation of alveolar bone dehiscences. An anatomical-radiological study--Part I. J Orofac Orthop. 1996 Apr;57(2):62-74.

32. Rothe LE, Bollen AM, Little RM, Herring SW, Chaison JB, Chen CS, Hollender LG. Trabecular and cortical bone as risk factors for orthodontic relapse. Am J Orthod Dentofacial Orthop. 2006 Oct;130(4):476-84.

33. Ericsson I, Thilander B. Orthodontic relapse in dentitions with reduced periodontal support: an experimental study in dogs. Eur J Orthod. 1980;2(1):51-7.

34. Melsen B, Allais D. Factors of importance for the development of dehiscences during labial movement of mandibular incisors: a retrospective study of adult orthodontic patients. Am J Orthod Dentofacial Orthop. 2005 May;127(5):552-61; quiz 625.

35. Wennstrom JL. Mucogingival considerations in orthodontic treatment. Semin Orthod. 1996 Mar;2(1):46-54.

36. Wennstrom JL, Lindhe J, Sinclair F, Thilander B. Some periodontal tissue reactions to orthodontic tooth movement in monkeys. J Clin Periodontol. 1987 Mar;14(3):121-9.

37. Yared KF, Zenobio EG, Pacheco W. Periodontal status of mandibular central incisors after orthodontic proclination in adults. Am J Orthod Dentofacial Orthop. 2006 Jul;130(1):6 e1-8.

38. Abdelmalek RG, Bissada NF. Incidence and distribution of alveolar bony dehiscence and fenestration in dry human Egyptian jaws. J Periodontol. 1973 Sep;44(9):586-8.

39. Davies RM, Downer MC, Hull PS, Lennon MA. Alveolar defects in human skulls. J Clin Periodontol. 1974;1(2):107-11.

40. Edel A. Alveolar bone fenestrations and dehiscences in dry Bedouin jaws. J Clin Periodontol. 1981 Dec;8(6):491-9.

41. Jorgic-Srdjak K, Plancak D, Bosnjak A, Azinovic Z. Incidence and distribution of dehiscences and fenestrations on human skulls. Coll Antropol. 1998 Dec;22 Suppl:111-6.

42. Larato DC. Alveolar plate fenestrations and dehiscences of the human skull. Oral Surg Oral Med Oral Pathol. 1970 Jun;29(6):816-9.

43. Rupprecht RD, Horning GM, Nicoll BK, Cohen ME. Prevalence of dehiscences and fenestrations in modern American skulls. J Periodontol. 2001 Jun;72(6):722-9.

44. Hulley S, Cummings S. Designing Clinical Research. 2nd ed. Philadelphia: Lippincott-Raven Publishers; 2001.

45. Araki K, Maki K, Seki K, Sakamaki K, Harata Y, Sakaino R, Okano T, Seo K. Characteristics of a newly developed dentomaxillofacial X-ray cone beam CT scanner (CB MercuRay): system configuration and physical properties. Dentomaxillofac Radiol. 2004 Jan;33(1):51-9.

46. Stahl S, Cantor M, Zwig E. Fenestrations of the Labial Alveolar Plate in Human Skulls. J Am Soc Periodontists. 1963;1(3):99-102.

47. Baumgaertel S, Palomo J, Palomo LB, Hans M. The Reliability and Accuracy of Dental Arch Measurements of Three Dimensional Cone Beam Computed Tomography Scans. Am J Orthod Dentofacial Orthop. (pending).

48. Mengel R, Kruse B, Flores-de-Jacoby L. Digital volume tomography in the diagnosis of peri-implant defects: an in vitro study on native pig mandibles. J Periodontol. 2006 Jul;77(7):1234-41.

49. Hilgers ML, Scarfe WC, Scheetz JP, Farman AG. Accuracy of linear temporomandibular joint measurements with cone beam computed tomography and digital cephalometric radiography. Am J Orthod Dentofacial Orthop. 2005 Dec;128(6):803-11.

50. Lascala CA, Panella J, Marques MM. Analysis of the accuracy of linear measurements obtained by cone beam computed tomography (CBCT-NewTom). Dentomaxillofac Radiol. 2004 Sep;33(5):291-4.

51. Hintze H, Wiese M, Wenzel A. Cone beam CT and conventional tomography for the detection of morphological temporomandibular joint changes. Dentomaxillofac Radiol. 2007 May;36(4):192-7.

52. Honda K, Larheim TA, Maruhashi K, Matsumoto K, Iwai K. Osseous abnormalities of the mandibular condyle: diagnostic reliability of cone beam computed tomography compared with helical computed tomography based on an autopsy material. Dentomaxillofac Radiol. 2006 May;35(3):152-7.

53. Ballrick J, Palomo J, Ruch E, Amberman B, Hans M. Image Distortion and Spatial Resolution of a Commercially Available CBCT. Am J Orthod Dentofacial Orthop. (pending).

54. Baba R, Ueda K, Kuba A, Kohda E, Shiraga N, Sanmiya T. Development of a subject-standing-type cone-beam computed tomography for chest and orthopedic imaging. Front Med Biol Eng. 2001;11(3):177-89.

55. Park HS, Lee YJ, Jeong SH, Kwon TG. Density of the alveolar and basal bones of the maxilla and the mandible. Am J Orthod Dentofacial Orthop. 2008 Jan;133(1):30-7.

56. Haaga JR, Miraldi F, MacIntyre W, LiPuma JP, Bryan PJ, Wiesen E. The effect of mAs variation upon computed tomography image quality as evaluated by in vivo and in vitro studies. Radiology. 1981 Feb;138(2):449-54.

57. Palomo J, Subramanyan K, Hans M. Influence of mA settings and a copper filter in CBCT image resolution. Int J Computer Assisted Radiology and Strategy. 2006;June(1):389-402.

58. Fuhrmann RA, Wehrbein H, Langen HJ, Diedrich PR. Assessment of the dentate alveolar process with high resolution computed tomography. Dentomaxillofac Radiol. 1995 Feb;24(1):50-4.

59. White S, Pharoah M. Oral Radiology: Principles and Interpretation. 4th ed. White S, editor. St. Louis: Mosby; 2000.

FIGURES AND TABLES

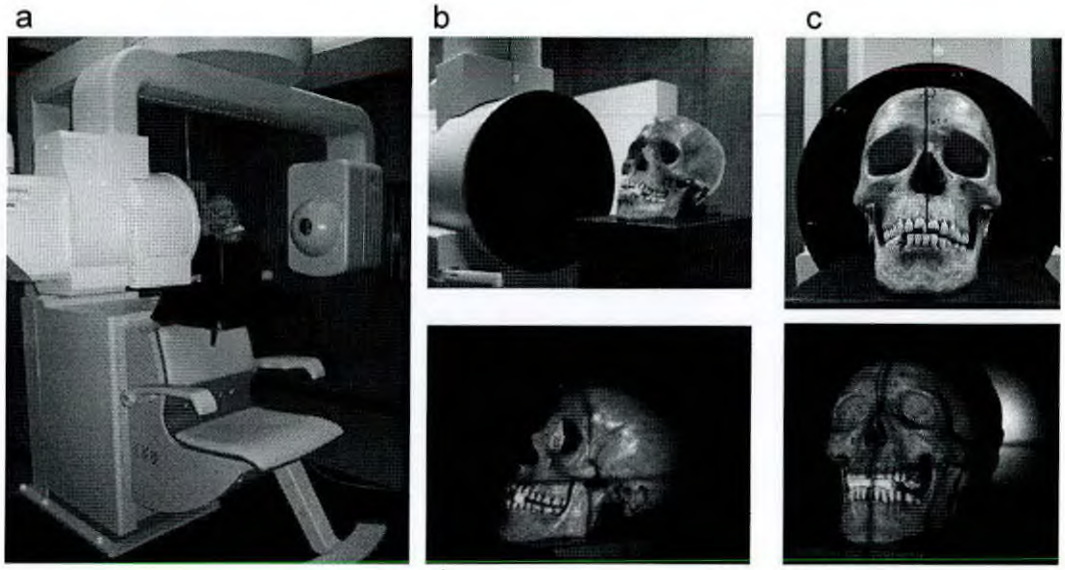


Figure 1. Positioning of skull for CBCT imaging

a) Overview of skull position with scanner
b) Lateral view of skull and detector placement
c) Frontal view of skull and detector placement
d) Lateral view of skull with lateral light positioning guides
e) Oblique view of skull with frontal light positioning guides

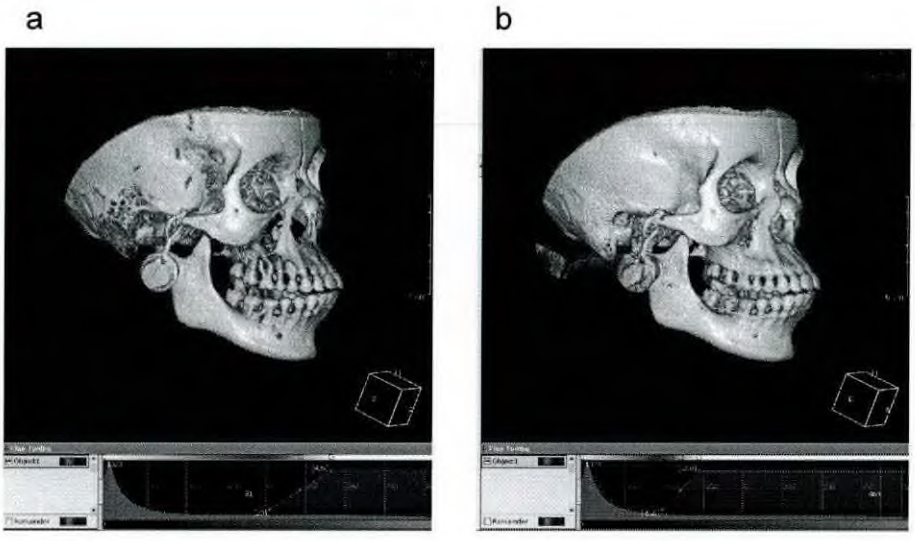


Figure 2. Illustration of 3D volume rendering and optimization
a) 3D volume rendering with manufacture-default density threshold set at 410 Hounsfield unit (HU) at the upper limit and 20 HU at the lower limit
b) 3D volume rendering with density threshold optimized by the operator at -280 HU at the upper and -510 HU at the lower limit

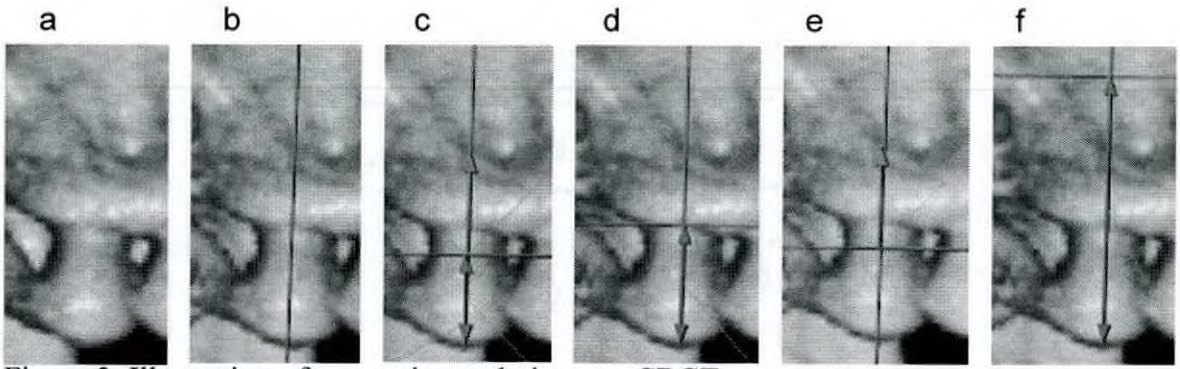


Figure 3. Illustration of measuring technique on CBCT

a) Tooth of interest with the buccal surface oriented squarely on screen
b) Tapeline drawn parallel to the long axis of the tooth
c) Measurement of T-CEJ from cusp tip to the most apical point on the CEJ along the long axis of the tooth
d) Measurement of T-BM from cusp tip to the most apical point on the bone margin along the long axis of the tooth
e) Measurement of T-Fen1 from cusp tip the most coronal border of a fenestration
f) Measurement of T-Fen2 from cusp tip to the most apical border of a fenestration

Table 1: Description of variables

Variables	*Description*
Dehiscence (Deh)	Buccal or facial alveolar bone defect involving the alveolar margin that is 3 mm or greater and concurrent with a "V" shape bone margin. Periodontal recessions involving the interproximal bone were excluded.
Fenestration (Fen)	A circumscribed defect on the buccal or facial alveolar bone exposing the root.
T-CEJ	The distance from the cusp tip to the cementoenamel junction (CEJ) parallel to the long axis of the tooth. Buccal cusps are used for posterior teeth and mid-incisal tips are used for anterior teeth.
T-BM	The distance from the cusp tip to the most coronal bone margin measured along a line parallel to the long axis of the tooth.
T-Fen1	The distance from the cusp tip to the most coronal border of a fenestration along a line parallel to the long axis of the tooth.
T-Fen2	The distance from the cusp tip to the most apical border of a fenestration along a line parallel to the long axis of the tooth.
Bone height	The distance obtained from taking the difference between the measurements T-CEJ and T-BM. The reference points were the same when a dehiscence was present.
Dehiscence height	The distance obtained from taking the difference between the measurements T-BM and T-CEJ.
Fenestration height	The distance obtained from taking the difference between the measurements T-Fen1 and T-Fen2.

Table 2: Distribution of teeth examined by tooth type

Tooth Type	Maxilla	Mandible	**Total**
Third molar	**17**	**7**	24
Second molar	**23**	**23**	46
First molar	**23**	**22**	45
Second Premolar	**25**	**23**	48
First Premolar	**22**	**25**	47
Cuspid	**21**	**21**	**42**
Lateral incisor	**22**	**23**	**45**
Central incisor	**14**	**23**	**37**
Total	**167**	**167**	**334**

Table 3: Measurement accuracy of T-CEJ and T-BM by means, mean differences, standard deviations, and correlations (n=446)

Variables	Direct $\bar{X}$ ±SD (mm)	CBCT $\bar{X}$ ±SD (mm)	Δ(Direct-CBCT) $\overline{\Delta}$ ±SD[a]	|Δ(Direct-CBCT)| $\overline{\lvert\Delta\rvert}$ ±SD[b]	Correlation	Sig.
T-CEJ	8.3±1.5	8.3±1.4	-0.1±0.5	0.4±0.3	0.941*	0.002**
T-BM	10.3±2.1	10.6±1.9	-0.2±1.0	0.6±0.8	0.871*	0.000**

[a]Mean difference between each direct and CBCT measurement.
[b]Mean of the absolute difference between each direct and CBCT measurement.
*Pearson correlaton coefficient is significant at the 0.01 level
**Paired two-tailed t-test is significant (P<0.01)

Table 4: Summary of Direct and CBCT results for the presence of dehiscence or fenestration by tooth type

		Direct		CBCT	
Tooth Type	**No. Of Sites**	**FEN**	**DEH**	**Fen**	Deh
Maxilla	***230***	***24***	***22***	***81***	*16*
Third Molar	**34**	**2**	**1**	**3**	1
Second Molar	**46**	**0**	**0**	**3**	0
First Molar	**46**	**12**	**6**	**32**	5
Second Premolar	**25**	**0**	**3**	**10**	1
First Premolar	**22**	**2**	**4**	**13**	4
Cuspid	**21**	**4**	**7**	**5**	4
Lateral Incisor	**22**	**3**	**0**	**9**	1
Central Incisor	**14**	**1**	**1**	**6**	0
Mandible	***216***	***8***	***30***	***23***	*27*
Third Molar	**13**	**0**	**0**	**0**	0
Second Molar	**44**	**0**	**1**	**0**	2
First Molar	**44**	**0**	**2**	**1**	3
Second Premolar	**23**	**1**	**1**	**4**	2
First Premolar	**25**	**2**	**7**	**2**	7
Cuspid	**21**	**1**	**5**	**7**	5
Lateral Incisor	**23**	**2**	**8**	**5**	6
Central Incisor	**23**	**2**	**6**	**4**	2
Total	446	32	52	104	43

Table 5: Detection of fenestrations and dehiscences by CBCT method versus Direct method

Fenestrations		Direct	
		FEN +	*FEN -*
CBCT	*fen +*	26	78
	fen -	6	336

Dehiscences		Direct	
		DEH +	*DEH -*
CBCT	*deh +*	22	21
	deh -	30	373

Table 6: Sensitivity and specificity of CBCT for detection of fenestrations and dehiscences

CBCT	Fenestration	**Dehiscence**
Sensitivity[a]	**0.81**	0.42
Specificity[b]	**0.81**	0.95
Positive Predictive Value[c]	**0.25**	0.51
Negative Predictive Value[d]	**0.98**	0.93

[a]Sensitivity is the probability of a positive test given the presence of the condition [a/(a+c)]. Sensitivity ≥ 0.80 is considered acceptable.
[b]Specificity is the probability of a negative test given the absence of the condition [d/(b+d)]. Specificity ≥ 0.80 is considered acceptable.
[c]Positive predictive value is the probability of the presence of the condition given a positive test result [a/(a+b)].
[d]Negative predictive value is the probability of the absence of the condition given a negative test result [d/(c+d)].

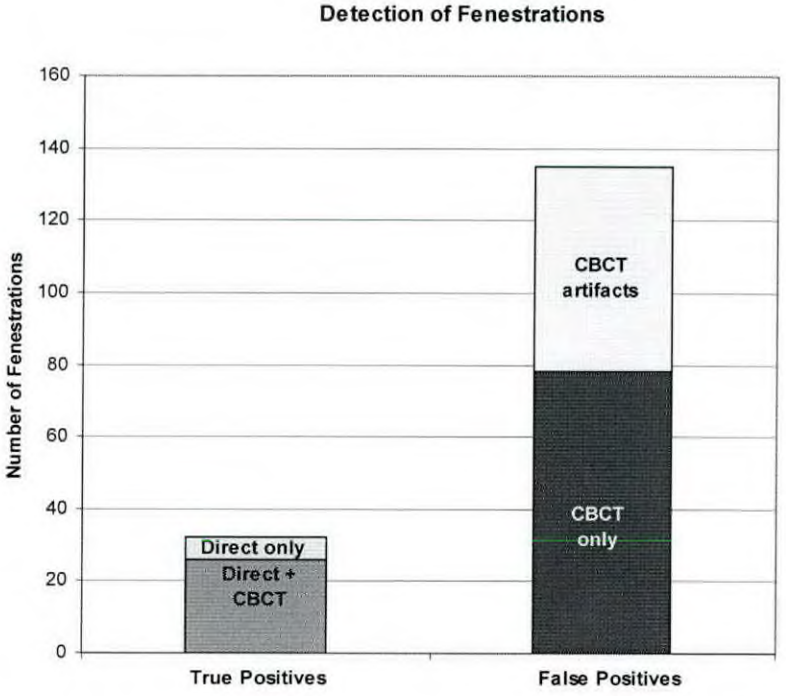


Figure 4. Histogram showing the number of fenestrations detected by direct and/or by CBCT methods. There were three times as many fenestrations detected by CBCT as compared to the direct method. The fenestrations detected on CBCT were considered artifacts if axial and/or coronal slice data showed presence of bone.

Table 7a: Analysis of dehiscence artifacts by cortical bone thickness

Cross Sections	No. Sites with Bone	$\bar{X}$ ±SD (mm)	Min[a]	Max[b]
Axial	18	0.8±0.2	0.6	1.2
Coronal	17	0.9±0.2	0.6	1.3

Table 7b: Analysis of fenestration artifacts by cortical bone thickness

Cross Sections	No. Sites with Bone	$\bar{X}$ ±SD (mm)	Min[a]	Max[b]
Axial	57	1.0±0.3	0.6	1.7
Coronal	56	1.0±0.2	0.7	1.7

[a]Minimum thickness of buccal cortical bone overlying root measured in millimeters
[b]Maximum thickness of buccal cortical bone overlying root measured in

Table 8: Intra-operator reliability for T-CEJ and T-BM measurements at timepoint 1 (T1) and timepoint 2 (T2) by means, mean differences, standard deviations, and intraclass correlation coefficient

	Direct			CBCT		
N=91	T1 $\bar{X}$ ±SD (mm)	T2 $\bar{X}$ ±SD (mm)	ICC[a]	T1 $\bar{X}$ ±SD (mm)	T2 $\bar{X}$ ±SD (mm)	ICC[a]
T-CEJ	8.2±1.6	8.3±1.5	0.987	7.9±1.6	8.0±1.6	0.948
T-BM	10.1±2.2	10.2±2.1	0.991	10.0±2.0	10.1±2.0	0.935

[a]Intraclass correlation coefficient.

Table 9: Intra-operator reliability for T-Fen1 and T-Fen2 measurements at timepoint 1 and timepoint 2 by means, mean differences, standard deviations, and intraclass correlation coefficient

	Direct			CBCT		
N=11	T1 $\bar{X}$ ±SD (mm)	T2 $\bar{X}$ ±SD (mm)	ICC[a]	T1 $\bar{X}$ ±SD (mm)	T2 $\bar{X}$ ±SD (mm)	ICC[a]
T-Fen1	14.9±2.0	14.8±2.1	0.992	14.1±3.2	14.0±2.8	0.937
T-Fen2	17.9±1.9	18.0±1.8	0.994	17.8±2.7	17.8±2.9	0.891

[a]Intraclass correlation coefficient.

APPENDIX I:

STATISTICS

TABLE 10:.--Descriptive statistics for CBCT tcejcA measurements

N	Valid	446
	Missing	0
	Mean	8.3300
	Std. Deviation	1.44889
	Skewness	.944
	Std. Error of Skewness	.116
	Kurtosis	.342
	Std. Error of Kurtosis	.231
	Range	7.00
	Minimum	5.58
	Maximum	12.58

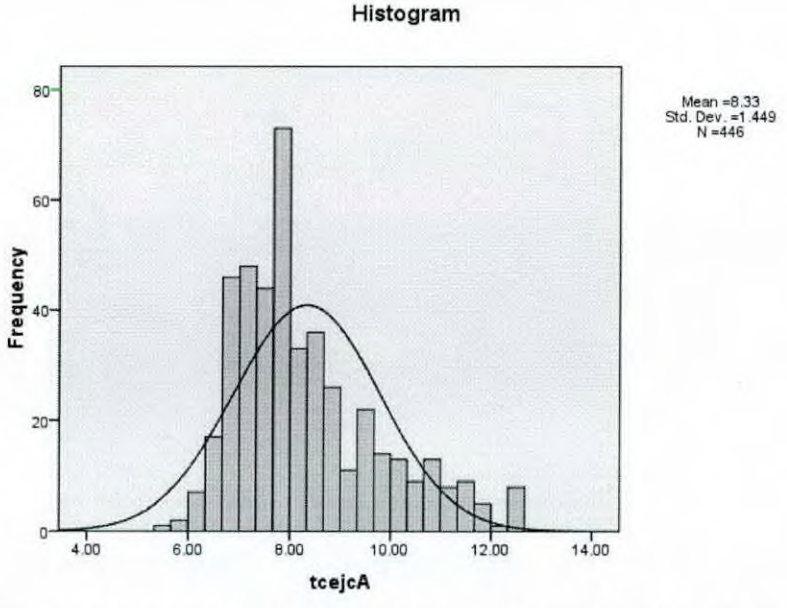


Figure 5. Evaluation of CBCT tcejcA measurements for normality. The frequency distribution indicates that the measurements are normally distributed.

TABLE 11.-- Descriptive statistics for CBCT tbmcA measurements

N	Valid	446
	Missing	0
	Mean	10.5598
	Std. Deviation	1.94531
	Skewness	.662
	Std. Error of Skewness	.116
	Kurtosis	-.188
	Std. Error of Kurtosis	.231
	Range	9.60
	Minimum	7.38
	Maximum	16.98

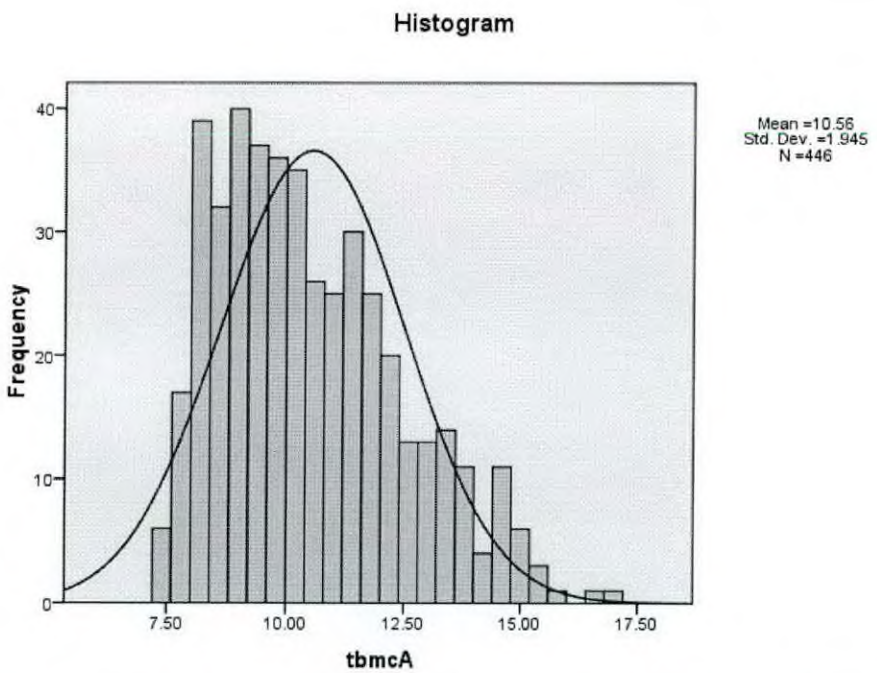


Figure 6. Evaluation of CBCT tbmcA measurements for normality. The frequency distribution indicates that the measurements are normally distributed.

TABLE 12.-- Descriptive statistics for Direct TCEJD measurements

N	Valid	446
	Missing	0
	Mean	8.2536
	Std. Deviation	1.48205
	Skewness	.918
	Std. Error of Skewness	.116
	Kurtosis	.157
	Std. Error of Kurtosis	.231
	Range	7.10
	Minimum	5.54
	Maximum	12.64

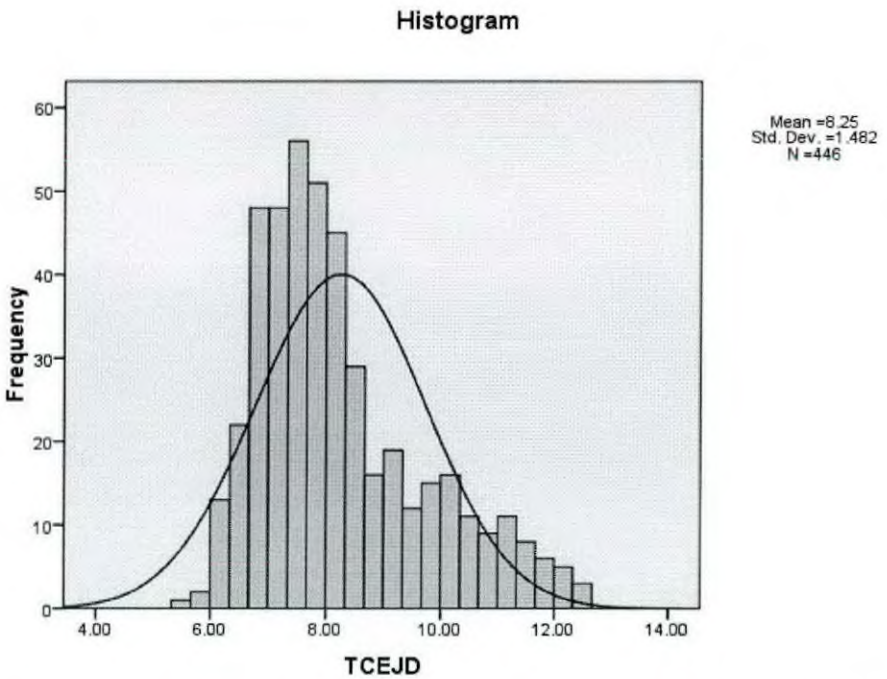


Figure 7. Evaluation of Direct TCEJD measurements for normality. The frequency distribution indicates that the measurements are normally distributed.

TABLE 13.—Descriptive statistics for Direct TBMD measurements

N	Valid	446
	Missing	0
	Mean	10.3436
	Std. Deviation	2.06184
	Skewness	.777
	Std. Error of Skewness	.116
	Kurtosis	.139
	Std. Error of Kurtosis	.231
	Range	10.33
	Minimum	6.64
	Maximum	16.97

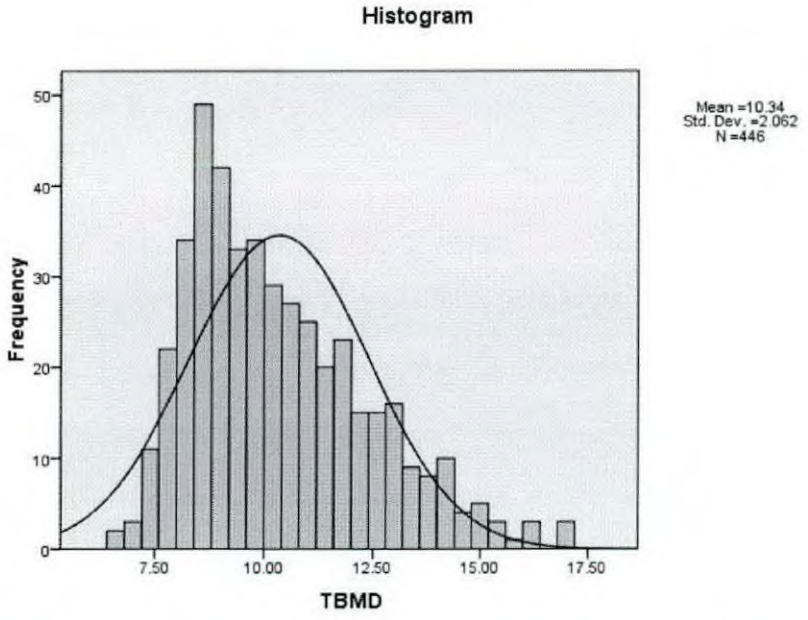


Figure 8. Evaluation of Direct TBMD measurements for normality. The frequency distribution indicates that the measurements are normally distributed.

TABLE 14.-- Paired Samples Statistics for Direct and CBCT T-CEJ Measurements

		Mean	N	Std. Deviation	Std. Error Mean
Pair 1	TCEJD	8.2536	446	1.48205	.07018
	tcejcA	8.3300	446	1.44889	.06861

TABLE 15.-- Paired Samples Correlations for Direct and CBCT T-CEJ Measurements

		N	Correlation	Sig.
Pair 1	TCEJD & tcejcA	446	.941	.000

**. Correlation is significant at the 0.01 level (2-tailed).

TABLE 16.-- Paired Samples Test for Direct and CBCT T-CEJ Measurements

		Paired Differences					t	df	Sig. (2-tailed)
		Mean	Std. Deviation	Std. Error Mean	95% Confidence Interval of the Difference				
					Lower	Upper			
Pair 1	TCEJD – tcejcA	-.07637	.50632	.02398	-.12349	-.02925	-3.185	445	.002

TABLE 17.-- Paired Samples Statistics for Direct and CBCT T-BM Measurements

		Mean	N	Std. Deviation	Std. Error Mean
Pair 1	TBMD	10.3436	446	2.06184	.09763
	tbmcA	10.5598	446	1.94531	.09211

TABLE 18.-- Paired Samples Correlations for Direct and CBCT T-BM Measurements

		N	Correlation	Sig.
Pair 1	TBMD & tbmcA	446	.871	.000

**. Correlation is significant at the 0.01 level (2-tailed).

TABLE 19.-- Paired Samples Test for Direct and CBCT T-BM Measurements

	Paired Differences					t	df	Sig. (2-tailed)
				95% Confidence Interval of the Difference				
	Mean	Std. Deviation	Std. Error Mean	Lower	Upper			
Pair 1 TBMD - tbmcA	-.21619	1.02256	.04842	-.31135	-.12103	-4.465	445	.000

TABLE 20.—Descriptive Statistics for Bone Thicknesses Measured on Slice Data on Excluded Dehiscences

	N	Minimum	Maximum	Mean	Std. Deviation
Axiald	18	.6	1.2	.828	.2024
Corond	17	.6	1.3	.894	.2331
Valid N (listwise)	17				

TABLE 21.--Descriptive Statistics for Bone Thicknesses Measured on Slice Data on Excluded Fenestrations

	N	Range	Minimum	Maximum	Mean	Std. Deviation
Axialf	57	1.1	.6	1.7	1.037	.2547
Coronf	56	1.0	.7	1.7	1.064	.2362
Valid N (listwise)	55					



TABLE 22.dehcA (Adjusted) * DEHD Crosstabulation

Count		DEHD		
		NO	YES	Total
dehcA	NO	328	23	351
	YES	66	29	95
	Total	394	52	446

TABLE 23.--dehc (Unadjusted)* DEHD Crosstabulation

Count		DEHD		
		NO	YES	Total
dehc	NO	357	28	385
	YES	37	24	61
	Total	394	52	446

TABLE 24.--fencA (Adjusted) * FEND

Crosstabulation

Count		FEND		
		NO	YES	Total
fencA	NO	336	6	342
	YES	78	26	104
	Total	414	32	446

TABLE 25.--fenc (unadjusted) * FEND

Crosstabulation

Count		FEND		
		NO	YES	Total
fenc	NO	279	6	285
	YES	135	26	161
	Total	414	32	446

INTRAEXAMINAR RELIABILITY

TABLE 26.--Descriptive Statistics for CBCT tcejc at Timepoint 1 and Timepoint 2

	N	Mean	Std. Deviation
tcejc1	91	7.871	1.6062
tcejc2	91	7.965	1.5536
Valid N (listwise)	91		

TABLE 27.--Intraclass Correlation Coefficient for CBCT tcejc at Timepoint 1 and Timepoint 2

	Intraclass Correlation[a]	95% Confidence Interval		F Test with True Value 0			
		Lower Bound	Upper Bound	Value	df1	df2	Sig
Single Measures	.935[b]	.903	.957	29.633	90	90	.000
Average Measures	.966[c]	.949	.978	29.633	90	90	.000

Two-way mixed effects model where people effects are random and measures effects are fixed.

a. Type A intraclass correlation coefficients using an absolute agreement definition.

b. The estimator is the same, whether the interaction effect is present or not.

c. This estimate is computed assuming the interaction effect is absent, because it is not estimable otherwise.

TABLE 28.--Descriptive Statistics for CBCT tbmc at Timepoint 1 and Timepoint 2

	N	Mean	Std. Deviation
tbmc1	91	10.000	2.0297
tbmc2	91	10.064	1.9622
Valid N (listwise)	91		

TABLE 29.--Intraclass Correlation Coefficient for CBCT tbmc at Timepoint 1 and Timepoint 2

	Intraclass Correlation[a]	95% Confidence Interval		F Test with True Value 0			
		Lower Bound	Upper Bound	Value	df1	df2	Sig
Single Measures	.937[b]	.866	.971	29.486	26	26	.000
Average Measures	.967[c]	.928	.985	29.486	26	26	.000

Two-way mixed effects model where people effects are random and measures effects are fixed.

a. Type A intraclass correlation coefficients using an absolute agreement definition.

b. The estimator is the same, whether the interaction effect is present or not.

c. This estimate is computed assuming the interaction effect is absent, because it is not estimable otherwise.

TABLE 30.--Descriptive Statistics for CBCT tfen1c at Timepoint 1 and Timepoint 2

	N	Mean	Std. Deviation
tfen1c1	27	14.078	3.1720
tfen1c2	36	13.675	2.6961
Valid N (listwise)	27		

TABLE 31.--Intraclass Correlation Coefficient for CBCT tfen1c at Timepoint 1 and Timepoint 2

	Intraclass Correlation[a]	95% Confidence Interval		F Test with True Value 0			
		Lower Bound	Upper Bound	Value	df1	df2	Sig
Single Measures	.937[b]	.866	.971	29.486	26	26	.000
Average Measures	.967[c]	.928	.985	29.486	26	26	.000

Two-way mixed effects model where people effects are random and measures effects are fixed.

a. Type A intraclass correlation coefficients using an absolute agreement definition.

b. The estimator is the same, whether the interaction effect is present or not.

c. This estimate is computed assuming the interaction effect is absent, because it is not estimable otherwise.

TABLE 32.--Descriptive Statistics for CBCT tfen2c at Timepoint 1 and Timepoint 2

	N	Mean	Std. Deviation
tfen2c1	27	17.848	2.6651
tfen2c2	36	17.394	2.9277
Valid N (listwise)	27		

TABLE 33.--Intraclass Correlation Coefficient for CBCT tfen2c at Timepoint 1 and Timepoint 2

	Intraclass Correlation[a]	95% Confidence Interval		F Test with True Value 0			
		Lower Bound	Upper Bound	Value	df1	df2	Sig
Single Measures	.891[b]	.776	.949	16.821	26	26	.000
Average Measures	.943[c]	.874	.974	16.821	26	26	.000

Two-way mixed effects model where people effects are random and measures effects are fixed.

a. Type A intraclass correlation coefficients using an absolute agreement definition.

b. The estimator is the same, whether the interaction effect is present or not.

c. This estimate is computed assuming the interaction effect is absent, because it is not estimable otherwise.

TABLE 34.--Descriptive Statistics for Direct TCEJD at Timepoint 1 and Timepoint 2

	N	Mean	Std. Deviation
TCEJD1	91	8.1886	1.58950
TCEJD2	91	8.2607	1.54881
Valid N (listwise)	91		

TABLE 35.--Intraclass Correlation Coefficient for Direct TCEJD at Timepoint 1 and Timepoint 2

	Intraclass Correlation[a]	95% Confidence Interval		F Test with True Value 0			
		Lower Bound	Upper Bound	Value	df1	df2	Sig
Single Measures	.987[b]	.980	.991	148.034	90	90	.000
Average Measures	.993[c]	.990	.996	148.034	90	90	.000

Two-way mixed effects model where people effects are random and measures effects are fixed.

a. Type C intraclass correlation coefficients using a consistency definition-the between-measure variance is excluded from the denominator variance.

b. The estimator is the same, whether the interaction effect is present or not.

c. This estimate is computed assuming the interaction effect is absent, because it is not estimable otherwise.

TABLE 36.--Descriptive Statistics for Direct TBMD at Timepoint 1 and Timepoint 2

	N	Minimum	Maximum	Mean	Std. Deviation
TBMD1	91	7.33	16.82	10.1377	2.16381
TBMD2	91	7.4	16.8	10.231	2.1055
Valid N (listwise)	91				

TABLE 37.—Intraclass Correlation Coefficient for Direct TBMD at Timepoint 1 and Timepoint 2

	Intraclass Correlation[a]	95% Confidence Interval		F Test with True Value 0			
		Lower Bound	Upper Bound	Value	df1	df2	Sig
Single Measures	.991[b]	.985	.995	256.089	90	90	.000
Average Measures	.996[c]	.993	.997	256.089	90	90	.000

Two-way mixed effects model where people effects are random and measures effects are fixed.

a. Type A intraclass correlation coefficients using an absolute agreement definition.

b. The estimator is the same, whether the interaction effect is present or not.

c. This estimate is computed assuming the interaction effect is absent, because it is not estimable otherwise.

TABLE 38.--Descriptive Statistics for Direct TFEN1D at Timepoint 1 and Timepoint 2

	N	Minimum	Maximum	Mean	Std. Deviation
TFEN1D1	11	12.21	18.41	14.9055	2.02505
TFEN1D2	11	11.82	18.35	14.8055	2.14986
Valid N (listwise)	11				

TABLE 39.--Intraclass Correlation Coefficient for Direct TFEN1D at Timepoint 1 and Timepoint 2

	Intraclass Correlation[a]	95% Confidence Interval		F Test with True Value 0			
		Lower Bound	Upper Bound	Value	df1	df2	Sig
Single Measures	.992[b]	.973	.998	278.217	10	10	.000
Average Measures	.996[c]	.986	.999	278.217	10	10	.000

Two-way mixed effects model where people effects are random and measures effects are fixed.

a. Type A intraclass correlation coefficients using an absolute agreement definition.

b. The estimator is the same, whether the interaction effect is present or not.

c. This estimate is computed assuming the interaction effect is absent, because it is not estimable otherwise.

TABLE 40.--Descriptive Statistics for Direct TFEN2D at Timepoint 1 and Timepoint 2

	N	Minimum	Maximum	Mean	Std. Deviation
TFEN2D1	11	15.45	20.78	17.9355	1.87208
TFEN2D2	11	15.57	20.64	17.9600	1.77976
Valid N (listwise)	11				

TABLE 41.--Intraclass Correlation Coefficient for Direct TFEN1D at Timepoint 1 and Timepoint 2

	Intraclass Correlation[a]	95% Confidence Interval		F Test with True Value 0			
		Lower Bound	Upper Bound	Value	df1	df2	Sig
Single Measures	.994[b]	.976	.998	284.216	10	10	.000
Average Measures	.997[c]	.988	.999	284.216	10	10	.000

Two-way mixed effects model where people effects are random and measures effects are fixed.

a. Type A intraclass correlation coefficients using an absolute agreement definition.

b. The estimator is the same, whether the interaction effect is present or not.

c. This estimate is computed assuming the interaction effect is absent, because it is not estimable otherwise.

APPENDIX II:

RAW DATA

TABLE A.--Abbreviations

Tooth ID	Unique identification given for each tooth (for molars point zero (0.0) refers to mesial cusps and point 1 (0.1) series refers to distal cusps)
Tooth No.	Tooth type identified with the Universal coding system (#1-32)
T-CEJD	Cusp tip to cementoenamel junction for the Direct method (in millimeter)
T-BMD	Cusp tip to bone margin for the Direct method (in millimeter)
T-FEN1D	Cusp tip to most coronal bone margin of a fenestration for the Direct method (in millimeter)
T-FEN2D	Cusp tip to most apical bone margin of a fenestration for the Direct method (in millimeter)
DEHD	Dehiscence by the Direct method (absent=0, present=1)
FEND	Fenestration by the Direct method (absent=0, present=1)
t-cejc	Cusp tip to cementoenamel junction for the CBCT method (in millimeter)
t-cejcA	Cusp tip to cementoenamel junction (t-cejc) adjusted for systematic error (in millimeter)
t-bmc	Cusp tip to bone margin for the CBCT method (in millimeter)
t-bmcA	Cusp tip to bone margin (t-bmc) adjusted for systematic error (in millimeter)
Dehc	Dehiscence by the CBCT method (absent=0, present=1)
dehcA	Dehiscence by the CBCT method after examining 2D slice data (absent=0, present=1)
t-fen1c	Cusp tip to most coronal bone margin of a fenestration for the CBCT method (in millimeter)
t-fen2c	Cusp tip to most apical bone margin of a fenestration for the CBCT method (in millimeter)
Fenc	Fenestration by the CBCT method (absent=0, present=1)
fencA	Fenestration by the CBCT method after examining 2D slice data (absent=0, present=1)
Bslice	Bone on slice data (absent=0, present=1)
Axial	Measurement of bone overlying root on axial slice (in millimeter)
Coronal	Measurement of bone overlying root on coronal slice (in millimeter)
	Note: Measurements for reliability tests are labeled as above followed by 1 for measurements taken at timepoint 1 and by 2 for measurements taken at timepoint 2.

TABLE B.--Raw and Adjusted Data from CBCT (accuracy)

Tooth ID	Tooth No.	t-cejc	t-cejcA	t-bm1c	tbm1cA	dehc	dehcA1	bsliced	axiald	corond	t-fen1c	t-fen2c	fenc	fencA	bslicef	axialf	coronf
1.0	1.0	6.3	6.68	7.8	8.18	0	0						0	0			
1.1	1.1	5.9	6.28	7.8	8.18	0	0				12.0	17.5	1	1	0	0.0	0.0
2.0	2.0	5.7	6.08	7.8	8.18	0	0						0	0			
2.1	2.1	5.6	5.98	7.7	8.08	0	0				14.8	18.3	1	1	0	0.0	0.0
3.0	3.0	5.9	6.28	7.7	8.08	0	0				12.3	15.8	1	1	0	0.0	0.0
3.1	3.1	5.6	5.98	7.6	7.98	0	0				13.5	17.0	1	1	0	0.0	0.0
4.0	4.0	6.1	6.48	7.5	7.88	0	0				14.0	19.0	1	1	0	0.0	0.0
5.0	5.0	7.1	7.48	9.2	9.58	0	0				13.1	18.6	1	1	0	0.0	0.0
6.0	6.0	9.1	9.48	11.6	11.98	0	0						0	0			
7.0	7.0	7.9	8.28	10.2	10.58	0	0						0	0			
8.0	10.0	8.6	8.98	10.2	10.58	0	0						0	0			
9.0	11.0	9.7	10.08	13.0	13.38	1	1	0	0.0	0.0			1	0	1	1.0	1.0
10.0	12.0	7.3	7.68	9.0	9.38	0	0				13.3	19.7	1	1	0	0.0	0.0
11.0	13.0	7.2	7.58	8.8	9.18	0	0						1	0	1	1.0	1.0
12.0	14.0	6.0	6.38	9.4	9.78	1	1	0	0.0	0.0	11.6	17.9	1	1	0	0.0	0.0
12.1	14.1	6.2	6.58	7.9	8.28	0	0				12.6	15.7	1	1	0	0.0	0.0
13.0	15.0	7.3	7.68	9.0	9.38	0	0						1	0	1	0.8	0.8
13.1	15.1	7.0	7.38	9.0	9.38	0	0						0	0			
14.0	16.0	6.6	6.98	8.5	8.88	0	0						1	0	1	1.0	1.0
14.1	16.1	6.1	6.48	7.9	8.28	0	0				14.0	16.9	1	1	0	0.0	0.0
15.0	17.0	6.7	7.08	7.8	8.18	0	0						0	0			
15.1	17.1	6.8	7.18	7.0	7.38	0	0						0	0			
16.0	18.0	7.3	7.68	9.2	9.58	0	0						0	0			
16.1	18.1	6.9	7.28	8.5	8.88	0	0						0	0			
17.0	19.0	5.7	6.08	8.2	8.58	0	0						0	0			
17.1	19.1	6.6	6.98	9.6	9.98	1	1	0	0.0	0.0			0	0			
18.0	20.0	7.9	8.28	9.1	9.48	0	0						0	0			
19.0	21.0	7.5	7.88	10.5	10.88	1	1	0	0.0	0.0			0	0			
20.0	23.0	8.3	8.68	10.8	11.18	0	0						0	0			
21.0	24.0	7.7	8.08	9.8	10.18	0	0						0	0			
22.0	25.0	7.9	8.28	9.6	9.98	0	0						0	0			
23.0	26.0	8.6	8.98	11.0	11.38	0	0						0	0			
24.0	28.0	6.9	7.28	10.9	11.28	1	1	0	0.0	0.0			0	0			
25.0	29.0	6.4	6.78	8.6	8.98	0	0						0	0			
26.0	30.0	7.0	7.38	9.2	9.58	0	0						0	0			
26.1	30.1	6.5	6.88	8.3	8.68	0	0						0	0			
27.0	31.0	5.2	5.58	8.0	8.38	0	0						0	0			
27.1	31.1	5.8	6.18	7.5	7.88	0	0						0	0			
28.0	32.0	6.0	6.38	7.9	8.28	0	0						0	0			
28.1	32.1	6.9	7.28	8.0	8.38	0	0						0	0			
29.0	1.0	7.6	7.98	9.4	9.78	0	0						0	0			
29.1	1.1	7.3	7.68	8.8	9.18	0	0						0	0			
30.0	2.0	7.8	8.18	9.5	9.88	0	0						0	0			
30.1	2.1	7.8	8.18	9.0	9.38	0	0						0	0			
31.0	4.0	7.7	8.08	9.6	9.98	0	0				16.7	22.8	1	1	0	0.0	0.0
32.0	5.0	8.4	8.78	10.5	10.88	0	0						0	0			
33.0	6.0	10.4	10.78	13.5	13.88	0	0						0	0			
34.0	7.0	10.1	10.48	12.4	12.78	0	0						0	0			
35.0	8.0	10.6	10.98	13.3	13.68	0	0						0	0			
36.0	9.0	10.6	10.98	12.9	13.28	0	0						0	0			

TABLE B.--Raw and Adjusted Data from CBCT (accuracy)

Tooth ID	Tooth No.	t-cejc	t-cejcA	t-bm1c	tbm1cA	dehc	dehcA1	bsliced	axiald	corond	t-fen1c	t-fen2c	fenc	fencA	bslicef	axialf	coronf
37.0	10.0	9.8	10.18	12.5	12.88	0	0						0	0			
38.0	11.0	9.5	9.88	11.5	11.88	0	0				18.7	21.4	1	1	0	0.0	0.0
39.0	12.0	9.0	9.38	11.1	11.48	0	0				18.1	22.4	1	1	0	0.0	0.0
40.0	13.0	8.0	8.38	9.9	10.28	0	0				14.3	16.6	1	1	0	0.0	0.0
41.0	15.0	7.4	7.78	9.7	10.08	0	0						0	0			
41.1	15.1	7.4	7.78	9.7	10.08	0	0						0	0			
42.0	16.0	7.6	7.98	9.1	9.48	0	0						0	0			
42.1	16.1	7.0	7.38	8.1	8.48	0	0						0	0			
43.0	18.0	8.3	8.68	10.5	10.88	0	0						0	0			
43.1	18.1	8.1	8.48	10.4	10.78	0	0						0	0			
44.0	20.0	8.5	8.88	10.3	10.68	0	0						0	0			
45.0	21.0	9.0	9.38	10.5	10.88	0	0						0	0			
46.0	22.0	10.6	10.98	13.0	13.38	0	0						0	0			
47.0	23.0	9.0	9.38	11.0	11.38	0	0						0	0	0	0.0	0.0
48.0	24.0	9.2	9.58	10.9	11.28	0	0						0	0			
49.0	25.0	8.7	9.08	11.0	11.38	0	0						0	0			
50.0	26.0	9.2	9.58	11.5	11.88	0	0						0	0	0	0.0	0.0
51.0	27.0	10.9	11.28	13.3	13.68	0	0						0	0			
52.0	28.0	8.7	9.08	10.6	10.98	0	0						0	0			
53.0	29.0	8.5	8.88	11.0	11.38	0	0						0	0			
54.0	31.0	7.8	8.18	10.1	10.48	0	0						0	0			
54.1	31.1	7.4	7.78	9.0	9.38	0	0						0	0			
55.0	1.0	6.5	6.88	8.8	9.18	0	0						1	0	1	1.2	1.2
55.1	1.1	6.0	6.38	7.7	8.08	0	0						1	0	1	1.2	1.2
56.0	2.0	6.6	6.98	8.6	8.98	0	0						0	0			
56.1	2.1	6.9	7.28	8.4	8.78	0	0						1	0	1	1.4	1.4
57.0	3.0	7.4	7.78	9.0	9.38	0	0				13.3	18.0	1	1	0	0.0	0.0
57.1	3.1	6.6	6.98	8.9	9.28	0	0				16.5	19.7	1	1	0	0.0	0.0
58.0	4.0	8.1	8.48	9.5	9.88	0	0						0	0			
59.0	5.0	8.0	8.38	10.5	10.88	0	0						0	0			
60.0	7.0	9.5	9.88	12.3	12.68	0	0				19.2	21.0	1	1	0	0.0	0.0
61.0	8.0	10.9	11.28	13.4	13.78	0	0						0	0			
62.0	9.0	11.2	11.58	14.1	14.48	0	0				22.0	24.4	1	1	0	0.0	0.0
63.0	10.0	9.5	9.88	12.6	12.98	1	0	1	0.8	0.7	16.2	19.0	1	1	0	0.0	0.0
64.0	11.0	10.8	11.18	13.2	13.58	0	0						0	0			
65.0	12.0	8.3	8.68	10.4	10.78	0	0						0	0			
66.0	13.0	7.5	7.88	9.6	9.98	0	0				19.4	21.3	1	1	0	0.0	0.0
67.0	14.0	6.4	6.78	12.6	12.98	1	1	0	0.0	0.0	13.6	18.8	1	1	0	0.0	0.0
67.1	14.1	6.3	6.68	8.6	8.98	0	0						0	0			
68.0	15.0	6.9	7.28	8.4	8.78	0	0						1	0	1	1.3	1.3
68.1	15.1	6.6	6.98	8.3	8.68	0	0						0	0			
69.0	16.0	6.0	6.38	7.0	7.38	0	0						1	0	1	1.7	1.7
69.1	16.1	5.9	6.28	7.3	7.68	0	0						0	0			
70.0	18.0	6.7	7.08	9.4	9.78	0	0						0	0			
70.1	18.1	6.9	7.28	7.4	7.78	0	0						0	0			
71.0	19.0	6.1	6.48	7.6	7.98	0	0						0	0			
71.1	19.1	6.3	6.68	7.1	7.48	0	0						0	0			
72.0	21.0	7.5	7.88	9.4	9.78	0	0						0	0			
73.0	22.0	11.2	11.58	14.3	14.68	1	1	0	0.0	0.0			0	0			
74.0	24.0	8.1	8.48	10.6	10.98	0	0						0	0			

TABLE B.--Raw and Adjusted Data from CBCT (accuracy)

Tooth ID	Tooth No.	t-cejc	t-cejcA	t-bm1c	tbm1cA	dehc	dehcA1	bsliced	axiald	corond	t-fen1c	t-fen2c	fenc	fencA	bslicef	axialf	coronf
75.0	25.0	7.6	7.98	10.4	10.78	0	0						0	0			
76.0	26.0	9.0	9.38	11.3	11.68	0	0						0	0			
77.0	27.0	11.0	11.38	14.5	14.88	1	1	0	0.0	0.0			0	0			
78.0	28.0	7.1	7.48	9.5	9.88	0	0						0	0			
79.0	30.0	5.9	6.28	7.3	7.68	0	0						0	0			
79.1	30.1	6.6	6.98	7.7	8.08	0	0						0	0			
80.0	31.0	6.9	7.28	7.5	7.88	0	0						0	0			
80.1	31.1	7.6	7.98	8.3	8.68	0	0						0	0			
81.0	3.0	7.4	7.78	11.7	12.08	0	0				16.0	19.2	1	1	0	0.0	0.0
81.1	3.1	7.5	7.88	12.0	12.38	0	0				13.1	18.7	1	1	0	0.0	0.0
82.0	4.0	7.5	7.88	10.4	10.78	0	0				16.1	22.0	1	1	0	0.0	0.0
83.0	5.0	8.5	8.88	11.0	11.38	0	0				20.9	24.3	1	1	0	0.0	0.0
84.0	6.0	10.2	10.58	14.1	14.48	1	1	0	0.0	0.0			0	0			
85.0	7.0	10.8	11.18	13.7	14.08	0	0				20.4	23.7	1	1	0	0.0	0.0
86.0	8.0	12.1	12.48	14.5	14.88	0	0						1	0	1	0.8	0.8
87.0	9.0	12.1	12.48	14.5	14.88	0	0				22.3	24.9	1	1	0	0.0	0.0
88.0	10.0	11.1	11.48	13.2	13.58	0	0						0	0			
89.0	11.0	11.4	11.78	14.5	14.88	0	0						0	0			
90.0	13.0	8.2	8.58	11.1	11.48	0	0				18.7	24.4	1	1	0	0.0	0.0
91.0	14.0	6.9	7.28	10.8	11.18	0	0				15.7	18.0	1	1	0	0.0	0.0
91.1	14.1	7.0	7.38	10.6	10.98	0	0				15.5	19.5	1	1	0	0.0	0.0
92.0	18.0	7.7	8.08	9.1	9.48	0	0						0	0			
92.1	18.1	8.0	8.38	9.2	9.58	0	0						0	0			
93.0	19.0	8.7	9.08	16.6	16.98	1	1	0	0.0	0.0			0	0			
93.1	19.1	8.5	8.88	11.2	11.58	0	0						0	0			
94.0	20.0	8.9	9.28	10.9	11.28	0	0				16.8	19.1	1	1	0	0.0	0.0
95.0	21.0	8.8	9.18	10.9	11.28	0	0						0	0			
96.0	22.0	11.2	11.58	12.9	13.28	0	0						0	0			
97.0	24.0	8.9	9.28	11.3	11.68	0	0				14.2	17.4	1	1	0	0.0	0.0
98.0	25.0	9.3	9.68	10.8	11.18	0	0				13.8	16.6	1	1	0	0.0	0.0
99.0	26.0	10.0	10.38	11.8	12.18	0	0				18.0	20.8	1	1	0	0.0	0.0
100.0	27.0	10.9	11.28	13.5	13.88	0	0				17.4	20.1	1	1	0	0.0	0.0
101.0	28.0	9.0	9.38	10.7	11.08	0	0						0	0			
102.0	29.0	8.5	8.88	11.0	11.38	0	0						0	0			
103.0	30.0	8.3	8.68	11.0	11.38	0	0						1	0	1	1.4	0.9
103.1	30.1	8.1	8.48	9.9	10.28	0	0						0	0			
104.0	31.0	7.4	7.78	12.5	12.88	1	1	0	0.0	0.0			0	0			
104.1	31.1	6.9	7.28	8.3	8.68	0	0						0	0			
105.0	1.0	6.9	7.28	8.0	8.38	0	0						0	0			
105.1	1.1	6.5	6.88	9.4	9.78	0	0						0	0			
106.0	2.0	7.6	7.98	12.7	13.08	1	0	1	0.9	1.3			0	0			
106.1	2.1	6.4	6.78	9.4	9.78	1	0	1	1.0	1.0	11.0	15.1	1	1	0	0.0	0.0
107.0	3.0	6.5	6.88	8.6	8.98	0	0						0	0			
107.1	3.1	6.6	6.98	9.4	9.78	0	0				14.3	17.4	1	1	0	0.0	0.0
108.0	4.0	7.9	8.28	14.1	14.48	1	1	0	0.0	0.0	16.6	20.4	1	1	0	0.0	0.0
109.0	5.0	9.4	9.78	13.5	13.88	1	1	0	0.0	0.0	17.2	19.2	1	1	0	0.0	0.0
110.0	6.0	10.5	10.88	15.0	15.38	1	1	0	0.0	0.0			0	0			
111.0	7.0	10.8	11.18	15.2	15.58	1	1	0	0.0	0.0			0	0			
112.0	12.0	8.8	9.18	12.7	13.08	1	1	0	0.0	0.0	13.8	16.1	1	1	0	0.0	0.0
113.0	13.0	7.6	7.98	11.1	11.48	1	0	1	1.1	1.1			1	0	1	0.7	0.7

TABLE B.--Raw and Adjusted Data from CBCT (accuracy)

Tooth ID	Tooth No.	t-cejc	t-cejcA	t-bm1c	tbm1cA	dehc	dehcA1	bsliced	axiald	corond	t-fen1c	t-fen2c	fenc	fencA	bslicef	axialf	coronf
114.0	14.0	7.7	8.08	12.3	12.68	1	1	0	0.0	0.0	14.2	17.9	1	1	0	0.0	0.0
114.1	14.1	7.2	7.58	9.9	10.28	0	0				11.9	18.8	1	1	0	0.0	0.0
115.0	15.0	8.1	8.48	10.4	10.78	0	0						1	0	1	0.7	0.7
115.1	15.1	7.1	7.48	9.9	10.28	0	0				13.0	17.3	1	1	0	0.0	0.0
116.0	16.0	6.7	7.08	8.1	8.48	0	0						1	0	1	1.6	1.6
116.1	16.1	7.2	7.58	10.3	10.68	1	1	0	0.0	0.0			0	0			
117.0	18.0	8.2	8.58	9.2	9.58	0	0						0	0			
117.1	18.1	7.9	8.28	8.5	8.88	0	0						0	0			
118.0	19.0	7.9	8.28	9.2	9.58	0	0						0	0			
118.1	19.1	8.2	8.58	10.0	10.38	0	0						0	0			
119.0	20.0	7.8	8.18	11.6	11.98	0	0						0	0			
120.0	21.0	9.9	10.28	12.2	12.58	0	0						0	0			
121.0	22.0	12.0	12.38	14.0	14.38	0	0						0	0			
122.0	23.0	10.5	10.88	12.0	12.38	0	0						0	0			
123.0	24.0	9.7	10.08	15.1	15.48	1	1	0	0.0	0.0			0	0			
124.0	25.0	9.2	9.58	11.0	11.38	0	0						0	0			
125.0	26.0	10.4	10.78	12.3	12.68	0	0						0	0			
126.0	27.0	12.0	12.38	14.1	14.48	0	0				16.2	18.4	1	1	0	0.0	0.0
127.0	28.0	9.2	9.58	11.9	12.28	0	0						0	0			
128.0	30.0	7.4	7.78	9.7	10.08	0	0						0	0			
128.1	30.1	7.5	7.88	10.0	10.38	0	0						0	0			
129.0	31.0	8.7	9.08	9.6	9.98	0	0						0	0			
129.1	31.1	7.9	8.28	9.1	9.48	0	0						0	0			
130.0	3.0	6.9	7.28	8.0	8.38	0	0						1	0	1	1.0	1.0
130.1	3.1	6.5	6.88	8.0	8.38	0	0				13.4	15.9	1	1	0	0.0	0.0
131.0	4.0	7.0	7.38	8.6	8.98	0	0						1	0	1	1.2	1.3
132.0	5.0	7.4	7.78	9.4	9.78	0	0						1	0	1	1.0	1.1
133.0	6.0	10.3	10.68	11.6	11.98	0	0				20.1	22.6	1	1	0	0.0	0.0
134.0	7.0	10.1	10.48	12.1	12.48	0	0				17.9	20.1	1	1	0	0.0	0.0
135.0	9.0	11.2	11.58	13.5	13.88	0	0				18.4	22.2	1	1	0	0.0	0.0
136.0	10.0	9.2	9.58	11.8	12.18	0	0				14.4	18.9	1	1	0	0.0	0.0
137.0	11.0	10.6	10.98	12.2	12.58	0	0				19.0	22.2	1	1	0	0.0	0.0
138.0	12.0	7.7	8.08	9.7	10.08	0	0						1	0	1	0.7	1.1
139.0	13.0	7.4	7.78	8.9	9.28	0	0						1	0	1	1.4	1.3
140.0	14.0	6.5	6.88	8.5	8.88	0	0				13.1	14.7	1	1	0	0.0	0.0
140.1	14.1	6.9	7.28	8.6	8.98	0	0				11.6	16.5	1	1	0	0.0	0.0
141.0	15.0	6.1	6.48	7.7	8.08	0	0						0	0			
141.1	15.1	6.6	6.98	7.6	7.98	0	0						0	0			
142.0	18.0	8.4	8.78	10.9	11.28	0	0						0	0			
142.1	18.1	8.0	8.38	8.6	8.98	0	0						1	0	1	0.9	0.9
143.0	19.0	6.7	7.08	7.4	7.78	0	0						0	0			
143.1	19.1	6.8	7.18	7.6	7.98	0	0						0	0			
144.0	20.0	6.0	6.38	11.0	11.38	1	1	0	0.0	0.0			0	0			
145.0	21.0	7.3	7.68	11.0	11.38	1	1	0	0.0	0.0			0	0			
146.0	22.0	9.7	10.08	11.5	11.88	0	0						0	0			
147.0	23.0	8.3	8.68	10.1	10.48	0	0						0	0			
148.0	24.0	8.0	8.38	10.3	10.68	0	0						0	0			
149.0	25.0	7.9	8.28	9.3	9.68	0	0						0	0			
150.0	26.0	8.5	8.88	9.6	9.98	0	0						0	0			
151.0	28.0	7.6	7.98	9.0	9.38	0	0						0	0			

TABLE B.--Raw and Adjusted Data from CBCT (accuracy)

Tooth ID	Tooth No.	t-cejc	t-cejcA	t-bm1c	tbm1cA	dehc	dehcA1	bsliced	axiald	corond	t-fen1c	t-fen2c	fenc	fencA	bslicef	axialf	coronf
152.0	29.0	7.3	7.68	9.2	9.58	0	0						0	0			
153.0	30.0	6.8	7.18	8.0	8.38	0	0						0	0			
153.1	30.1	7.4	7.78	8.6	8.98	0	0						0	0			
154.0	31.0	7.9	8.28	8.9	9.28	0	0						0	0			
154.1	31.1	8.1	8.48	9.0	9.38	0	0						0	0			
155.0	1.0	6.1	6.48	7.6	7.98	0	0						1	0	1	1.0	1.0
155.1	1.1	6.3	6.68	13.2	13.58	1	0	1	0.8	0.9			0	0			
156.0	2.0	6.8	7.18	8.3	8.68	0	0						0	0			
156.1	2.1	7.0	7.38	8.2	8.58	0	0						0	0			
157.0	3.0	7.4	7.78	9.2	9.58	0	0				11.9	15.5	1	1	0	0.0	0.0
157.1	3.1	7.6	7.98	9.2	9.58	0	0				13.4	16.3	1	1	0	0.0	0.0
158.0	4.0	7.7	8.08	9.4	9.78	0	0						0	0			
159.0	5.0	8.2	8.58	10.1	10.48	0	0				15.9	22.2	1	1	0	0.0	0.0
160.0	6.0	11.3	11.68	12.1	12.48	0	0						0	0			
161.0	7.0	10.3	10.68	11.5	11.88	0	0						0	0			
162.0	8.0	11.0	11.38	12.5	12.88	0	0				20.4	22.0	1	1	0	0.0	0.0
163.0	9.0	11.3	11.68	12.6	12.98	0	0						0	0			
164.0	10.0	9.6	9.98	11.5	11.88	0	0				15.2	17.4	1	1	0	0.0	0.0
165.0	11.0	11.3	11.68	13.1	13.48	0	0						0	0			
166.0	12.0	8.3	8.68	11.4	11.78	1	1	0	0.0	0.0			0	0			
167.0	13.0	8.1	8.48	9.6	9.98	0	0						0	0			
168.0	14.0	7.2	7.58	9.9	10.28	0	0				12.0	16.1	1	1	0	0.0	0.0
168.1	14.1	7.3	7.68	9.8	10.18	0	0						0	0			
169.0	15.0	7.2	7.58	8.7	9.08	0	0						0	0			
169.1	15.1	6.7	7.08	8.8	9.18	0	0						0	0			
170.0	16.0	6.9	7.28	8.6	8.98	0	0						0	0			
170.1	16.1	6.5	6.88	8.3	8.68	0	0						1	0	1	1.0	1.0
171.0	17.0	6.8	7.18	7.8	8.18	0	0						0	0			
171.1	17.1	6.9	7.28	7.3	7.68	0	0						0	0			
172.0	18.0	7.5	7.88	7.9	8.28	0	0						0	0			
172.1	18.1	7.6	7.98	7.9	8.28	0	0						0	0			
173.0	19.0	6.3	6.68	7.2	7.58	0	0						0	0			
173.1	19.1	6.7	7.08	7.4	7.78	0	0						0	0			
174.0	20.0	7.6	7.98	9.5	9.88	0	0						0	0			
175.0	21.0	8.4	8.78	9.2	9.58	0	0						0	0			
176.0	22.0	11.2	11.58	12.6	12.98	0	0						0	0			
177.0	23.0	9.7	10.08	11.3	11.68	0	0						0	0			
178.0	24.0	9.4	9.78	11.2	11.58	0	0						0	0			
179.0	25.0	9.0	9.38	10.7	11.08	0	0						0	0			
180.0	26.0	9.8	10.18	11.7	12.08	0	0						0	0			
181.0	27.0	11.0	11.38	13.4	13.78	0	0						0	0			
182.0	28.0	8.1	8.48	10.0	10.38	0	0						0	0			
183.0	29.0	6.8	7.18	8.8	9.18	0	0						0	0			
184.0	30.0	6.4	6.78	7.4	7.78	0	0						0	0			
184.1	30.1	6.6	6.98	7.2	7.58	0	0						0	0			
185.0	31.0	7.4	7.78	8.0	8.38	0	0						0	0			
185.1	31.1	7.6	7.98	8.1	8.48	0	0						0	0			
186.0	1.0	6.3	6.68	8.3	8.68	0	0						0	0			
186.1	1.1	6.3	6.68	8.4	8.78	0	0						0	0			
187.0	2.0	7.1	7.48	8.8	9.18	0	0						0	0			

TABLE B.--Raw and Adjusted Data from CBCT (accuracy)

Tooth ID	Tooth No.	t-cejc	t-cejcA	t-bm1c	tbm1cA	dehc	dehcA1	bsliced	axiald	corond	t-fen1c	t-fen2c	fenc	fencA	bslicef	axialf	coronf
187.1	2.1	6.4	6.78	9.2	9.58	0	0						0	0			
188.0	4.0	6.7	7.08	12.2	12.58	1	0	1	0.9	0.9	16.9	18.7	1	1	0	0.0	0.0
189.0	5.0	7.7	8.08	10.4	10.78	0	0				11.5	14.9	1	1	0	0.0	0.0
190.0	6.0	10.1	10.48	14.5	14.88	1	1	0	0.0	0.0			0	0			
191.0	7.0	9.8	10.18	12.2	12.58	0	0						0	0			
192.0	10.0	10.0	10.38	12.5	12.88	0	0				16.4	20.8	1	1	0	0.0	0.0
193.0	11.0	10.3	10.68	13.0	13.38	0	0				20.2	22.1	1	1	0	0.0	0.0
194.0	12.0	8.0	8.38	10.5	10.88	0	0				16.2	20.4	1	1	0	0.0	0.0
195.0	13.0	6.6	6.98	8.4	8.78	0	0				11.5	13.8	1	1	1	1.6	1.6
196.0	14.0	6.3	6.68	9.7	10.08	0	0				13.3	17.0	1	1	0	0.0	0.0
196.1	14.1	6.0	6.38	9.3	9.68	0	0				11.6	15.9	1	1	0	0.0	0.0
197.0	15.0	7.3	7.68	8.0	8.38	0	0						0	0			
197.1	15.1	6.3	6.68	7.5	7.88	0	0						0	0			
198.0	18.0	7.3	7.68	8.2	8.58	0	0						0	0			
198.1	18.1	7.0	7.38	7.8	8.18	0	0						0	0			
199.0	19.0	6.9	7.28	8.0	8.38	0	0						0	0			
199.1	19.1	7.0	7.38	7.9	8.28	0	0						0	0			
200.0	20.0	6.1	6.48	9.6	9.98	0	0						0	0			
201.0	21.0	8.2	8.58	9.8	10.18	0	0						0	0			
202.0	22.0	10.0	10.38	13.0	13.38	1	1	0	0.0	0.0			0	0			
203.0	23.0	8.4	8.78	10.7	11.08	0	0						0	0			
204.0	24.0	7.7	8.08	10.1	10.48	0	0						0	0			
205.0	25.0	7.7	8.08	9.7	10.08	0	0						0	0			
206.0	26.0	8.7	9.08	10.6	10.98	0	0						0	0			
207.0	27.0	10.0	10.38	12.0	12.38	0	0				14.4	18.0	1	1	0	0.0	0.0
208.0	28.0	8.1	8.48	10.5	10.88	0	0						0	0			
209.0	29.0	6.8	7.18	9.5	9.88	0	0						0	0			
210.0	30.0	6.7	7.08	8.5	8.88	0	0						0	0			
210.1	30.1	6.8	7.18	9.2	9.58	0	0						0	0			
211.0	31.0	7.3	7.68	8.6	8.98	0	0						0	0			
211.1	31.1	7.1	7.48	7.9	8.28	0	0						0	0			
212.0	2.0	6.1	6.48	8.0	8.38	0	0						1	0	1	1.4	1.4
212.1	2.1	6.0	6.38	8.5	8.88	0	0						1	0	1	1.1	1.2
213.0	3.0	6.3	6.68	8.8	9.18	0	0						1	0	1	0.7	0.8
213.1	3.1	6.4	6.78	9.3	9.68	0	0						1	0	1	0.9	1.0
214.0	4.0	8.2	8.58	11.1	11.48	0	0						1	0	1	1.4	1.4
215.0	8.0	12.1	12.48	15.6	15.98	1	0	1	0.6	0.6			1	0	1	1.1	1.1
216.0	9.0	12.2	12.58	14.2	14.58	0	0						1	0	1	0.8	0.8
217.0	10.0	11.3	11.68	13.2	13.58	0	0				16.6	20.7	1	1	0	0.0	0.0
218.0	12.0	9.2	9.58	11.8	12.18	0	0						1	0	1	0.8	0.8
219.0	13.0	7.8	8.18	9.8	10.18	0	0						1	0	1	1.0	1.1
220.0	14.0	6.5	6.88	8.1	8.48	0	0						1	0	1	1.0	1.0
220.1	14.1	6.7	7.08	8.7	9.08	0	0						0	0			
221.0	15.0	7.6	7.98	8.5	8.88	0	0						0	0			
221.1	15.1	6.9	7.28	8.0	8.38	0	0						0	0			
222.0	18.0	7.6	7.98	8.8	9.18	0	0						1	0	1	1.4	1.4
223.0	19.0	7.6	7.98	9.0	9.38	0	0						0	0			
223.1	19.1	7.2	7.58	9.1	9.48	0	0						0	0			
224.0	20.0	8.4	8.78	10.8	11.18	0	0						1	0	1	0.7	0.0
225.0	21.0	9.9	10.28	12.0	12.38	0	0						0	0			

TABLE B.--Raw and Adjusted Data from CBCT (accuracy)

Tooth ID	Tooth No.	t-cejc	t-cejcA	t-bm1c	tbm1cA	dehc	dehcA1	bsliced	axiald	corond	t-fen1c	t-fen2c	fenc	fencA	bslicef	axialf	coronf
226.0	22.0	11.9	12.28	14.4	14.78	0	0						0	0			
227.0	23.0	10.3	10.68	11.4	11.78	0	0						0	0			
228.0	25.0	9.9	10.28	10.9	11.28	0	0						0	0			
229.0	26.0	9.7	10.08	11.3	11.68	0	0						0	0			
230.0	27.0	12.1	12.48	13.8	14.18	0	0						0	0			
231.0	28.0	8.5	8.88	11.0	11.38	0	0						0	0			
232.0	29.0	6.3	6.68	8.0	8.38	0	0						0	0			
233.0	30.0	6.9	7.28	8.0	8.38	0	0						1	0	1	0.0	0.8
233.1	30.1	6.5	6.88	7.8	8.18	0	0						0	0			
234.0	31.0	7.1	7.48	8.2	8.58	0	0						0	0			
235.0	1.0	7.2	7.58	10.8	11.18	0	0						0	0			
235.1	1.1	6.9	7.28	10.0	10.38	0	0						1	0	1	1.1	1.1
236.0	2.0	8.7	9.08	10.1	10.48	0	0						0	0			
236.1	2.1	8.6	8.98	10.7	11.08	0	0						1	0	1	0.9	0.9
237.0	3.0	7.0	7.38	10.3	10.68	1	1	0	0.0	0.0	15.3	17.1	1	1	0	0.0	0.0
237.1	3.1	6.9	7.28	11.0	11.38	1	0	1	1.1	1.1			0	0			
238.0	4.0	7.2	7.58	10.0	10.38	0	0				17.9	19.6	1	1	0	0.0	0.0
239.0	5.0	8.2	8.58	11.0	11.38	0	0				18.0	19.8	1	1	0	0.0	0.0
240.0	6.0	8.9	9.28	11.9	12.28	1	0	1	0.7	0.6			0	0			
241.0	7.0	9.6	9.98	12.4	12.78	0	0						0	0			
242.0	9.0	10.7	11.08	13.8	14.18	0	0						0	0			
243.0	10.0	9.4	9.78	11.9	12.28	0	0						0	0			
244.0	11.0	9.0	9.38	11.3	11.68	0	0						0	0			
245.0	14.0	8.3	8.68	10.1	10.48	0	0				15.8	18.0	1	1	0	0.0	0.0
245.1	14.1	8.4	8.78	10.1	10.48	0	0						0	0			
246.0	15.0	8.0	8.38	10.8	11.18	0	0						0	0			
246.1	15.1	6.9	7.28	10.1	10.48	0	0						0	0			
247.0	17.0	7.5	7.88	8.4	8.78	0	0						0	0			
247.1	17.1	6.6	6.98	7.0	7.38	0	0						0	0			
248.0	19.0	7.1	7.48	8.8	9.18	0	0						0	0			
248.1	19.1	7.2	7.58	8.6	8.98	0	0						0	0			
249.0	20.0	7.5	7.88	10.5	10.88	1	0	1	0.7	0.7			0	0			
250.0	21.0	7.5	7.88	9.7	10.08	0	0						0	0			
251.0	22.0	9.8	10.18	11.7	12.08	0	0						0	0			
252.0	23.0	8.1	8.48	14.3	14.68	1	1	0	0.0	0.0			0	0			
253.0	24.0	9.1	9.48	11.5	11.88	0	0						0	0			
254.0	25.0	8.1	8.48	12.1	12.48	0	0						0	0			
255.0	26.0	9.1	9.48	13.2	13.58	1	1	0	0.0	0.0			0	0			
256.0	27.0	10.0	10.38	11.5	11.88	0	0						0	0			
257.0	28.0	7.3	7.68	11.1	11.48	1	1	0	0.0	0.0			0	0			
258.0	29.0	7.2	7.58	9.7	10.08	0	0						0	0			
259.0	30.0	7.4	7.78	10.4	10.78	1	0	1	0.6	0.8			0	0			
259.1	30.1	7.6	7.98	8.1	8.48	0	0						0	0			
260.0	32.0	7.5	7.88	8.0	8.38	0	0						0	0			
260.1	32.1	7.2	7.58	7.8	8.18	0	0						0	0			
261.0	1.0	6.9	7.28	9.4	9.78	0	0						1	0	1	0.7	0.7
261.1	1.1	6.0	6.38	9.6	9.98	0	0						1	0	1	0.7	0.7
262.0	2.0	7.0	7.38	9.8	10.18	0	0						1	0	1	0.9	0.9
262.1	2.1	6.1	6.48	9.0	9.38	0	0						0	0			
263.0	3.0	7.2	7.58	11.4	11.78	0	0				12.8	16.6	1	1	0	0.0	0.0

TABLE B.--Raw and Adjusted Data from CBCT (accuracy)

Tooth ID	Tooth No.	t-cejc	t-cejcA	t-bm1c	tbm1cA	dehc	dehcA1	bsliced	axiald	corond	t-fen1c	t-fen2c	fenc	fencA	bslicef	axialf	coronf
263.1	3.1	6.9	7.28	11.6	11.98	0	0						0	0			
264.0	4.0	7.4	7.78	9.4	9.78	0	0						1	0	1	1.0	1.2
265.0	7.0	10.5	10.88	13.2	13.58	0	0						0	0			
266.0	8.0	12.1	12.48	14.2	14.58	0	0				16.7	21.9	1	1	0	0.0	0.0
267.0	11.0	9.2	9.58	11.7	12.08	0	0						0	0			
268.0	12.0	7.2	7.58	9.5	9.88	0	0				13.8	17.5	1	1	0	0.0	0.0
269.0	13.0	7.2	7.58	9.8	10.18	0	0						0	0			
270.0	14.0	7.5	7.88	9.9	10.28	0	0						0	0			
270.1	14.1	7.8	8.18	10.1	10.48	0	0				14.3	17.7	1	1	0	0.0	0.0
271.0	15.0	7.5	7.88	9.7	10.08	0	0						1	0	1	1.2	1.2
271.1	15.1	6.8	7.18	8.8	9.18	0	0						1	0	1	0.9	1.0
272.0	17.0	6.9	7.28	8.0	8.38	0	0						0	0			
272.1	17.1	6.7	7.08	7.7	8.08	0	0						0	0			
273.0	18.0	6.5	6.88	7.9	8.28	0	0						0	0			
273.1	18.1	6.3	6.68	7.6	7.98	0	0						0	0			
274.0	19.0	6.3	6.68	8.3	8.68	0	0						0	0			
274.1	19.1	6.4	6.78	8.1	8.48	0	0						0	0			
275.0	20.0	7.4	7.78	9.0	9.38	0	0						0	0			
276.0	21.0	7.9	8.28	10.4	10.78	0	0						0	0			
277.0	22.0	9.5	9.88	12.5	12.88	1	1	0	0.0	0.0	13.7	21.6	1	1	0	0.0	0.0
278.0	23.0	8.1	8.48	14.6	14.98	1	1	0	0.0	0.0			0	0			
279.0	24.0	9.1	9.48	11.7	12.08	0	0						0	0			
280.0	25.0	8.4	8.78	11.6	11.98	1	1	0	0.0	0.0			0	0			
281.0	26.0	8.2	8.58	13.5	13.88	1	1	0	0.0	0.0	14.4	18.1	1	1	0	0.0	0.0
282.0	27.0	9.6	9.98	11.5	11.88	0	0				12.7	17.0	1	1	0	0.0	0.0
283.0	28.0	7.5	7.88	10.9	11.28	1	1	0	0.0	0.0			0	0			
284.0	29.0	7.4	7.78	9.8	10.18	0	0						0	0			
285.0	31.0	7.8	8.18	11.0	11.38	1	1	0	0.0	0.0			0	0			
285.1	31.1	7.3	7.68	8.3	8.68	0	0						0	0			
286.0	32.0	6.9	7.28	7.9	8.28	0	0						0	0			
287.0	1.0	7.4	7.78	8.4	8.78	0	0						1	0	1	1.0	1.0
287.1	1.1	7.2	7.58	8.6	8.98	0	0				10.4	14.5	1	1	0	0.0	0.0
288.0	2.0	7.2	7.58	8.4	8.78	0	0						0	0			
288.1	2.1	7.0	7.38	8.4	8.78	0	0						0	0			
289.0	3.0	6.3	6.68	9.6	9.98	0	0				11.2	16.6	1	1	0	0.0	0.0
289.1	3.1	7.0	7.38	10.0	10.38	0	0				11.4	17.2	1	1	0	0.0	0.0
290.0	4.0	7.7	8.08	9.0	9.38	0	0						0	0			
291.0	5.0	7.5	7.88	9.6	9.98	0	0				10.0	14.0	1	1	0	0.0	0.0
292.0	6.0	9.1	9.48	11.1	11.48	0	0				12.8	19.3	1	1	0	0.0	0.0
293.0	7.0	9.4	9.78	13.3	13.68	1	0	1	0.6	0.7	14.7	16.3	1	1	0	0.0	0.0
294.0	8.0	10.9	11.28	14.2	14.58	1	0	1	0.6	0.0	16.3	19.6	1	1	0	0.0	0.0
295.0	10.0	9.5	9.88	11.4	11.78	0	0						0	0			
296.0	11.0	9.8	10.18	11.9	12.28	0	0						0	0			
297.0	12.0	7.6	7.98	12.4	12.78	1	1	0	0.0	0.0	13.6	16.6	1	1	0	0.0	0.0
298.0	13.0	7.4	7.78	11.1	11.48	1	0	1	0.6	0.7			1	0	1	0.8	0.9
299.0	14.0	6.3	6.68	10.2	10.58	1	1	0	0.0	0.0	11.0	16.1	1	1	0	0.0	0.0
299.1	14.1	6.6	6.98	8.5	8.88	0	0				10.1	14.6	1	1	0	0.0	0.0
300.0	15.0	7.1	7.48	8.3	8.68	0	0						1	0	1	1.1	1.1
300.1	15.1	6.6	6.98	7.9	8.28	0	0						1	0	1	1.1	1.2
301.0	16.0	7.4	7.78	10.5	10.88	0	0						0	0			

TABLE B.--Raw and Adjusted Data from CBCT (accuracy)

Tooth ID	Tooth No.	t-cejc	t-cejcA	t-bm1c	tbm1cA	dehc	dehcA1	bsliced	axiald	corond	t-fen1c	t-fen2c	fenc	fencA	bslicef	axialf	coronf
301.1	16.1	7.2	7.58	10.1	10.48	0	0						0	0			
302.0	18.0	8.1	8.48	9.1	9.48	0	0						0	0			
302.1	18.1	7.8	8.18	8.5	8.88	0	0						0	0			
303.0	19.0	7.1	7.48	8.6	8.98	0	0						0	0			
303.1	19.1	6.6	6.98	10.5	10.88	1	1	0	0.0	0.0			0	0			
304.0	20.0	7.0	7.38	13.6	13.98	1	1	0	0.0	0.0			0	0			
305.0	21.0	7.8	8.18	8.9	9.28	0	0				11.5	17.1	1	1	0	0.0	0.0
306.0	23.0	7.5	7.88	9.3	9.68	0	0				11.4	16.8	1	1	0	0.0	0.0
307.0	24.0	7.9	8.28	9.8	10.18	0	0				11.4	15.4	1	1	0	0.0	0.0
308.0	25.0	7.9	8.28	9.5	9.88	0	0				11.7	15.8	1	1	0	0.0	0.0
309.0	28.0	8.3	8.68	14.4	14.78	1	1	0	0.0	0.0			0	0			
310.0	29.0	7.2	7.58	9.7	10.08	0	0				10.6	15.2	1	1	0	0.0	0.0
311.0	31.0	7.5	7.88	12.6	12.98	1	0	1	1.2	1.3			0	0			
311.1	31.1	8.1	8.48	8.9	9.28	0	0						0	0			
312.0	1.0	7.3	7.68	8.8	9.18	0	0						1	0	1	0.8	1.0
312.1	1.1	6.9	7.28	8.6	8.98	0	0						1	0	1	0.9	0.9
313.0	2.0	7.4	7.78	8.2	8.58	0	0						0	0			
313.1	2.1	7.3	7.68	8.1	8.48	0	0						0	0			
314.0	3.0	7.6	7.98	8.8	9.18	0	0				9.8	15.2	1	1	0	0.0	0.0
314.1	3.1	7.3	7.68	8.6	8.98	0	0						0	0			
315.0	4.0	6.9	7.28	9.7	10.08	0	0						1	0	1	1.2	1.2
316.0	5.0	8.1	8.48	11.5	11.88	1	0	1	0.8	0.8			0	0			
317.0	6.0	9.2	9.58	11.7	12.08	0	0						0	0			
318.0	7.0	8.1	8.48	13.2	13.58	1	0	1	0.8	0.8			1	0	1	0.6	0.8
319.0	11.0	9.0	9.38	11.6	11.98	0	0						0	0			
320.0	12.0	8.2	8.58	10.7	11.08	0	0						0	0			
321.0	13.0	7.9	8.28	9.2	9.58	0	0						1	0	1	1.1	1.2
322.0	14.0	7.5	7.88	9.5	9.88	0	0				14.1	17.2	1	1	0	0.0	0.0
322.1	14.1	6.9	7.28	8.6	8.98	0	0						1	0	1	1.2	1.2
323.0	15.0	8.4	8.78	10.1	10.48	0	0						1	0	1	1.1	1.1
323.1	15.1	8.2	8.58	9.9	10.28	0	0						1	0	1	1.0	0.0
324.0	16.0	7.6	7.98	8.9	9.28	0	0						1	0	1	0.8	0.8
324.1	16.1	7.2	7.58	16.1	16.48	1	0	1	1.1	1.2			1	0	1	1.1	1.1
325.0	19.0	6.8	7.18	8.2	8.58	0	0						0	0			
325.1	19.1	7.0	7.38	8.4	8.78	0	0						0	0			
326.0	20.0	7.6	7.98	9.4	9.78	0	0				12.0	14.5	1	1	0	0.0	0.0
327.0	22.0	9.0	9.38	11.9	12.28	0	0				13.9	16.8	1	1	0	0.0	0.0
328.0	23.0	8.2	8.58	12.0	12.38	1	1	0	0.0	0.0	13.4	17.8	1	1	0	0.0	0.0
329.0	26.0	8.1	8.48	12.0	12.38	1	1	0	0.0	0.0	14.3	16.7	1	1	0	0.0	0.0
330.0	27.0	9.4	9.78	12.5	12.88	1	1	0	0.0	0.0	14.4	16.8	1	1	0	0.0	0.0
331.0	28.0	7.5	7.88	11.5	11.88	1	1	0	0.0	0.0	14.6	19.1	1	1	0	0.0	0.0
332.0	29.0	6.7	7.08	9.9	10.28	0	0				10.9	14.7	1	1	0	0.0	0.0
333.0	30.0	7.2	7.58	9.4	9.78	0	0				10.1	12.5	1	1	0	0.0	0.0
333.1	30.1	7.2	7.58	8.6	8.98	0	0						0	0			
334.0	31.0	7.8	8.18	9.8	10.18	0	0						0	0			
334.1	31.1	8.0	8.38	10.0	10.38	0	0						0	0			

TABLE C.--Raw Data from Direct (accuracy)

Tooth ID	Tooth No.	T-CEJD	T-BMD	T-FEN1D	T-FEN2D	DEHD	FEND
1.0	1.0	6.49	8.21			0	0
1.1	1.1	6.57	8.19	15.68	17.22	0	1
2.0	2.0	6.79	8.31			0	0
2.1	2.1	6.40	7.98			0	0
3.0	3.0	6.54	8.32			0	0
3.1	3.1	6.71	7.65			0	0
4.0	4.0	6.42	8.19			0	0
5.0	5.0	7.05	9.70	16.33	19.95	0	1
6.0	6.0	9.74	12.85			1	0
7.0	7.0	9.09	11.63			0	0
8.0	10.0	9.34	11.27			0	0
9.0	11.0	9.81	13.15			1	0
10.0	12.0	6.83	9.37			0	0
11.0	13.0	5.90	9.03			1	0
12.0	14.0	5.82	9.54			1	0
12.1	14.1	6.26	9.21			0	0
13.0	15.0	6.85	9.30			0	0
13.1	15.1	6.90	8.42			0	0
14.0	16.0	6.14	8.22			0	0
14.1	16.1	6.26	7.57	13.85	16.99	0	1
15.0	17.0	6.69	7.24			0	0
15.1	17.1	6.06	6.64			0	0
16.0	18.0	7.01	9.46			0	0
16.1	18.1	6.45	8.94			0	0
17.0	19.0	6.49	8.83			0	0
17.1	19.1	6.14	9.46			0	0
18.0	20.0	6.63	9.98			0	0
19.0	21.0	7.83	10.52			0	0
20.0	23.0	9.09	12.72			1	0
21.0	24.0	7.89	10.26			0	0
22.0	25.0	8.02	10.44			0	0
23.0	26.0	8.90	11.94			1	0
24.0	28.0	7.89	11.09			1	0
25.0	29.0	6.85	9.35			0	0
26.0	30.0	6.53	8.59			0	0
26.1	30.1	6.77	8.25			0	0
27.0	31.0	7.27	9.05			0	0
27.1	31.1	6.87	8.16			0	0
28.0	32.0	6.24	6.69			0	0
28.1	32.1	6.24	6.88			0	0
29.0	1.0	7.48	9.13			0	0
29.1	1.1	7.31	8.93			0	0
30.0	2.0	8.20	9.66			0	0
30.1	2.1	7.83	9.38			0	0
31.0	4.0	8.10	9.87			0	0

TABLE C.--Raw Data from Direct (accuracy)

Tooth ID	Tooth No.	T-CEJD	T-BMD	T-FEN1D	T-FEN2D	DEHD	FEND
32.0	5.0	9.02	10.63			0	0
33.0	6.0	10.80	14.06			1	0
34.0	7.0	10.52	12.00			0	0
35.0	8.0	11.06	12.89			0	0
36.0	9.0	10.37	12.55			0	0
37.0	10.0	10.46	12.15			0	0
38.0	11.0	10.21	11.79	20.05	23.53	0	1
39.0	12.0	9.09	11.49			0	0
40.0	13.0	8.38	10.45			0	0
41.0	15.0	7.80	10.65			0	0
41.1	15.1	7.99	9.62			0	0
42.0	16.0	6.94	8.49			0	0
42.1	16.1	6.68	8.38			0	0
43.0	18.0	7.74	9.91			0	0
43.1	18.1	7.73	9.97			0	0
44.0	20.0	8.30	10.26			0	0
45.0	21.0	8.81	11.44			0	0
46.0	22.0	10.79	12.35			0	0
47.0	23.0	9.13	10.80			0	0
48.0	24.0	8.80	10.80			0	0
49.0	25.0	9.09	10.85			0	0
50.0	26.0	9.28	11.56			0	0
51.0	27.0	10.87	13.64			0	0
52.0	28.0	8.77	10.82			0	0
53.0	29.0	8.36	11.63			0	0
54.0	31.0	7.83	9.99			0	0
54.1	31.1	7.94	9.34			0	0
55.0	1.0	6.95	8.42			0	0
55.1	1.1	6.17	7.38			0	0
56.0	2.0	7.14	8.89			0	0
56.1	2.1	7.35	8.58			0	0
57.0	3.0	6.69	9.42	15.91	17.89	0	1
57.1	3.1	7.18	9.49			0	0
58.0	4.0	8.16	9.55			0	0
59.0	5.0	8.60	10.76			0	0
60.0	7.0	9.58	12.28			0	0
61.0	8.0	11.33	13.60			0	0
62.0	9.0	11.20	13.40			0	0
63.0	10.0	9.80	12.51	18.41	20.46	0	1
64.0	11.0	11.38	14.87			1	0
65.0	12.0	8.59	10.92			0	0
66.0	13.0	8.05	9.87			0	0
67.0	14.0	6.91	10.07	15.70	19.06	1	1
67.1	14.1	7.26	9.46			0	0
68.0	15.0	7.31	9.18			0	0

TABLE C.--Raw Data from Direct (accuracy)

Tooth ID	Tooth No.	T-CEJD	T-BMD	T-FEN1D	T-FEN2D	DEHD	FEND
68.1	15.1	8.10	8.43			0	0
69.0	16.0	6.30	7.21			0	0
69.1	16.1	6.10	6.88			0	0
70.0	18.0	7.89	8.32			0	0
70.1	18.1	7.44	7.93			0	0
71.0	19.0	6.38	7.71			0	0
71.1	19.1	6.20	7.33			0	0
72.0	21.0	8.46	10.50			0	0
73.0	22.0	11.87	15.39			1	0
74.0	24.0	8.31	11.26			0	0
75.0	25.0	8.44	10.87			0	0
76.0	26.0	9.54	11.89			0	0
77.0	27.0	11.35	15.57			1	0
78.0	28.0	8.16	10.56			0	0
79.0	30.0	6.97	7.82			0	0
79.1	30.1	6.60	7.91			0	0
80.0	31.0	7.68	8.72			0	0
80.1	31.1	7.27	8.11			0	0
81.0	3.0	7.49	11.78	16.21	19.38	1	1
81.1	3.1	7.76	11.62	14.57	19.65	1	1
82.0	4.0	8.61	10.82			0	0
83.0	5.0	8.87	11.06			0	0
84.0	6.0	10.90	13.83			0	0
85.0	7.0	11.69	14.15			0	0
86.0	8.0	12.07	15.24			1	0
87.0	9.0	12.18	15.08			0	0
88.0	10.0	11.68	14.34			0	0
89.0	11.0	11.57	14.28			0	0
90.0	13.0	8.51	11.67			1	0
91.0	14.0	7.38	10.74			0	0
91.1	14.1	7.61	10.35	15.66	19.96	0	1
92.0	18.0	9.03	9.99			0	0
92.1	18.1	7.87	8.70			0	0
93.0	19.0	8.79	16.12			1	0
93.1	19.1	8.24	11.02			0	0
94.0	20.0	9.22	10.92	13.98	18.40	0	1
95.0	21.0	9.16	11.02	14.91	20.78	0	1
96.0	22.0	11.63	13.68			0	0
97.0	24.0	9.32	10.99	16.48	18.85	0	1
98.0	25.0	9.47	11.36	15.91	18.49	0	1
99.0	26.0	10.27	12.37	17.11	22.42	0	1
100.0	27.0	11.66	12.97			0	0
101.0	28.0	9.43	11.09	17.31	18.74	0	1
102.0	29.0	8.91	11.54			0	0
103.0	30.0	8.56	11.51			0	0

TABLE C.--Raw Data from Direct (accuracy)

Tooth ID	Tooth No.	T-CEJD	T-BMD	T-FEN1D	T-FEN2D	DEHD	FEND
103.1	30.1	8.02	10.06			0	0
104.0	31.0	7.65	11.70			1	0
104.1	31.1	7.20	8.46			0	0
105.0	1.0	7.02	7.61			0	0
105.1	1.1	7.22	7.95			0	0
106.0	2.0	7.91	9.56			0	0
106.1	2.1	7.50	8.75			0	0
107.0	3.0	7.12	9.97			0	0
107.1	3.1	7.41	10.28			0	0
108.0	4.0	8.06	10.56			0	0
109.0	5.0	9.39	12.84			1	0
110.0	6.0	11.76	14.03			0	0
111.0	7.0	11.49	13.36			0	0
112.0	12.0	8.98	11.90			0	0
113.0	13.0	8.24	10.56			0	0
114.0	14.0	7.49	10.39			0	0
114.1	14.1	7.63	9.89			0	0
115.0	15.0	8.24	10.16			0	0
115.1	15.1	7.62	9.06			0	0
116.0	16.0	7.51	7.88			0	0
116.1	16.1	7.21	7.83			0	0
117.0	18.0	8.34	9.28			0	0
117.1	18.1	7.77	8.68			0	0
118.0	19.0	7.92	9.55			0	0
118.1	19.1	8.16	10.00			0	0
119.0	20.0	8.46	10.89			0	0
120.0	21.0	9.98	12.88			0	0
121.0	22.0	12.15	14.82			0	0
122.0	23.0	10.57	12.39			0	0
123.0	24.0	9.80	16.97			1	0
124.0	25.0	9.46	11.57			0	0
125.0	26.0	10.41	12.51			0	0
126.0	27.0	12.30	14.88			0	0
127.0	28.0	9.72	12.87			1	0
128.0	30.0	7.77	10.23			0	0
128.1	30.1	7.81	10.02			0	0
129.0	31.0	8.27	9.64			0	0
129.1	31.1	8.16	8.81			0	0
130.0	3.0	7.04	8.13			0	0
130.1	3.1	7.06	8.16			0	0
131.0	4.0	7.43	8.89			0	0
132.0	5.0	8.33	9.47			0	0
133.0	6.0	10.71	11.90			0	0
134.0	7.0	10.14	11.45	17.91	18.99	0	1
135.0	9.0	11.27	13.50			0	0

TABLE C.--Raw Data from Direct (accuracy)

Tooth ID	Tooth No.	T-CEJD	T-BMD	T-FEN1D	T-FEN2D	DEHD	FEND
136.0	10.0	9.87	11.22			0	0
137.0	11.0	10.96	12.34			0	0
138.0	12.0	7.90	9.47			0	0
139.0	13.0	7.58	8.89			0	0
140.0	14.0	7.09	8.87			0	0
140.1	14.1	7.07	8.24			0	0
141.0	15.0	7.87	8.56			0	0
141.1	15.1	7.50	8.04			0	0
142.0	18.0	8.19	8.93			0	0
142.1	18.1	7.51	8.40			0	0
143.0	19.0	7.41	8.76			0	0
143.1	19.1	7.34	8.62			0	0
144.0	20.0	7.37	8.75			0	0
145.0	21.0	8.05	9.90			0	0
146.0	22.0	10.56	12.44			0	0
147.0	23.0	8.40	10.60			0	0
148.0	24.0	8.29	10.95			0	0
149.0	25.0	7.96	9.99			0	0
150.0	26.0	8.62	10.29			0	0
151.0	28.0	8.18	9.68			0	0
152.0	29.0	7.72	8.63			0	0
153.0	30.0	7.48	8.78			0	0
153.1	30.1	7.40	8.55			0	0
154.0	31.0	8.07	9.03			0	0
154.1	31.1	7.62	8.08			0	0
155.0	1.0	6.73	8.44			0	0
155.1	1.1	6.38	7.81			0	0
156.0	2.0	6.93	8.57			0	0
156.1	2.1	6.75	8.42			0	0
157.0	3.0	6.49	9.38			0	0
157.1	3.1	6.78	8.92			0	0
158.0	4.0	7.25	9.05			0	0
159.0	5.0	8.04	10.75			0	0
160.0	6.0	10.93	12.91	15.80	18.94	0	1
161.0	7.0	10.20	11.91			0	0
162.0	8.0	11.31	13.08	15.48	16.18	0	1
163.0	9.0	11.22	13.14			0	0
164.0	10.0	9.73	11.77			0	0
165.0	11.0	11.12	13.05			0	0
166.0	12.0	7.85	10.85			0	0
167.0	13.0	7.11	9.34			0	0
168.0	14.0	6.68	9.92			1	0
168.1	14.1	6.70	9.04			0	0
169.0	15.0	7.27	8.63			0	0
169.1	15.1	6.09	9.00			0	0

TABLE C.--Raw Data from Direct (accuracy)

Tooth ID	Tooth No.	T-CEJD	T-BMD	T-FEN1D	T-FEN2D	DEHD	FEND
170.0	16.0	6.75	8.16			0	0
170.1	16.1	6.02	7.27			0	0
171.0	17.0	7.17	7.80			0	0
171.1	17.1	6.35	6.82			0	0
172.0	18.0	7.63	8.67			0	0
172.1	18.1	7.47	8.21			0	0
173.0	19.0	6.74	7.53			0	0
173.1	19.1	6.76	7.57			0	0
174.0	20.0	7.67	9.07			0	0
175.0	21.0	8.48	10.77			0	0
176.0	22.0	11.51	13.96			0	0
177.0	23.0	9.85	12.95			1	0
178.0	24.0	9.47	12.41			0	0
179.0	25.0	9.41	12.54			1	0
180.0	26.0	10.26	14.18			1	0
181.0	27.0	11.78	14.08			0	0
182.0	28.0	8.76	10.92			0	0
183.0	29.0	7.78	9.10			0	0
184.0	30.0	7.31	7.91			0	0
184.1	30.1	6.89	7.78			0	0
185.0	31.0	7.91	8.62			0	0
185.1	31.1	7.28	7.78			0	0
186.0	1.0	7.23	8.55			0	0
186.1	1.1	5.54	8.20			0	0
187.0	2.0	6.83	8.51			0	0
187.1	2.1	6.80	8.54			0	0
188.0	4.0	6.80	10.79			1	0
189.0	5.0	7.46	10.20			0	0
190.0	6.0	10.29	12.74			0	0
191.0	7.0	10.40	12.89			0	0
192.0	10.0	10.40	13.27			0	0
193.0	11.0	10.18	13.55			1	0
194.0	12.0	8.42	11.21	17.66	20.63	0	1
195.0	13.0	7.38	9.04			0	0
196.0	14.0	6.45	10.35			0	0
196.1	14.1	6.45	10.40	14.95	15.87	0	1
197.0	15.0	6.96	8.17			0	0
197.1	15.1	6.54	7.73			0	0
198.0	18.0	7.10	8.25			0	0
198.1	18.1	6.85	7.74			0	0
199.0	19.0	7.14	8.08			0	0
199.1	19.1	6.75	8.36			0	0
200.0	20.0	7.63	9.08			0	0
201.0	21.0	8.21	10.30			0	0
202.0	22.0	11.06	13.79			0	0

TABLE C.--Raw Data from Direct (accuracy)

Tooth ID	Tooth No.	T-CEJD	T-BMD	T-FEN1D	T-FEN2D	DEHD	FEND
203.0	23.0	8.74	11.24			0	0
204.0	24.0	7.71	10.28			0	0
205.0	25.0	7.85	9.96			0	0
206.0	26.0	8.73	11.96			0	0
207.0	27.0	11.16	14.23			1	0
208.0	28.0	8.18	10.38			0	0
209.0	29.0	6.53	8.87			0	0
210.0	30.0	7.30	8.79			0	0
210.1	30.1	7.11	9.42			0	0
211.0	31.0	7.52	7.88			0	0
211.1	31.1	6.55	7.33			0	0
212.0	2.0	7.24	8.26			0	0
212.1	2.1	6.84	7.73			0	0
213.0	3.0	6.89	9.36			0	0
213.1	3.1	6.63	9.21			0	0
214.0	4.0	8.02	9.93			0	0
215.0	8.0	12.09	14.10			0	0
216.0	9.0	12.35	13.93			0	0
217.0	10.0	11.65	12.67			0	0
218.0	12.0	9.49	10.78			0	0
219.0	13.0	8.19	10.26			0	0
220.0	14.0	6.63	8.76			0	0
220.1	14.1	7.35	8.72			0	0
221.0	15.0	7.83	8.51			0	0
221.1	15.1	7.81	8.43			0	0
222.0	18.0	8.48	9.01			0	0
223.0	19.0	7.72	8.99			0	0
223.1	19.1	7.11	8.72			0	0
224.0	20.0	8.61	10.73			0	0
225.0	21.0	9.77	12.61			0	0
226.0	22.0	12.60	14.87			0	0
227.0	23.0	10.04	11.43			0	0
228.0	25.0	10.00	11.55			0	0
229.0	26.0	10.21	11.74			0	0
230.0	27.0	12.64	14.48	16.91	18.36	0	1
231.0	28.0	8.98	10.81			0	0
232.0	29.0	8.50	9.36			0	0
233.0	30.0	7.15	8.66			0	0
233.1	30.1	6.82	8.17			0	0
234.0	31.0	8.36	8.98			0	0
235.0	1.0	7.88	9.89			0	0
235.1	1.1	7.23	9.60			0	0
236.0	2.0	8.04	10.42			0	0
236.1	2.1	7.53	10.23			0	0
237.0	3.0	7.38	10.11	15.45	16.67	0	1

TABLE C.--Raw Data from Direct (accuracy)

Tooth ID	Tooth No.	T-CEJD	T-BMD	T-FEN1D	T-FEN2D	DEHD	FEND
237.1	3.1	6.86	9.74			0	0
238.0	4.0	8.10	10.08			0	0
239.0	5.0	8.44	10.74			0	0
240.0	6.0	9.46	12.08			0	0
241.0	7.0	9.98	11.98			0	0
242.0	9.0	11.17	13.58			0	0
243.0	10.0	9.83	12.25			0	0
244.0	11.0	8.96	11.87			0	0
245.0	14.0	7.73	9.82			0	0
245.1	14.1	7.13	9.76			0	0
246.0	15.0	7.94	10.36			0	0
246.1	15.1	6.87	9.37			0	0
247.0	17.0	7.15	8.00			0	0
247.1	17.1	6.71	7.28			0	0
248.0	19.0	7.31	8.93			0	0
248.1	19.1	7.19	8.37			0	0
249.0	20.0	8.08	11.18			0	0
250.0	21.0	7.78	10.53			0	0
251.0	22.0	10.00	12.45			0	0
252.0	23.0	8.69	11.50			0	0
253.0	24.0	8.66	11.88			1	0
254.0	25.0	9.11	12.16			1	0
255.0	26.0	9.06	11.96			0	0
256.0	27.0	10.03	13.78			1	0
257.0	28.0	8.35	11.69			1	0
258.0	29.0	8.12	9.93			0	0
259.0	30.0	7.47	8.92			0	0
259.1	30.1	7.03	8.37			0	0
260.0	32.0	7.14	7.67			0	0
260.1	32.1	6.37	7.31			0	0
261.0	1.0	7.56	10.19			0	0
261.1	1.1	6.83	9.95			1	0
262.0	2.0	7.51	10.83			0	0
262.1	2.1	7.14	9.77			0	0
263.0	3.0	7.11	11.72			0	0
263.1	3.1	6.79	10.22			0	0
264.0	4.0	7.62	10.95			0	0
265.0	7.0	10.83	12.77			0	0
266.0	8.0	11.83	14.44			0	0
267.0	11.0	10.35	12.60			0	0
268.0	12.0	7.97	10.25			0	0
269.0	13.0	7.49	9.69			0	0
270.0	14.0	7.45	10.56			0	0
270.1	14.1	7.74	10.66			0	0
271.0	15.0	6.91	9.60			0	0

TABLE C.--Raw Data from Direct (accuracy)

Tooth ID	Tooth No.	T-CEJD	T-BMD	T-FEN1D	T-FEN2D	DEHD	FEND
271.1	15.1	6.82	8.67			0	0
272.0	17.0	7.40	8.20			0	0
272.1	17.1	7.27	8.49			0	0
273.0	18.0	7.76	8.69			0	0
273.1	18.1	7.14	8.27			0	0
274.0	19.0	6.98	8.29			0	0
274.1	19.1	7.15	8.76			0	0
275.0	20.0	8.03	9.46			0	0
276.0	21.0	8.23	10.68			0	0
277.0	22.0	10.63	13.18			0	0
278.0	23.0	9.21	14.74			1	0
279.0	24.0	9.19	12.25			1	0
280.0	25.0	8.46	11.89			1	0
281.0	26.0	9.30	14.51			1	0
282.0	27.0	10.77	12.14			0	0
283.0	28.0	8.19	11.49			1	0
284.0	29.0	8.21	10.91			0	0
285.0	31.0	8.38	11.27			0	0
285.1	31.1	7.89	8.88			0	0
286.0	32.0	7.61	8.16			0	0
287.0	1.0	7.36	8.27			0	0
287.1	1.1	7.42	8.50			0	0
288.0	2.0	7.43	7.89			0	0
288.1	2.1	7.25	8.31			0	0
289.0	3.0	6.87	8.95	12.91	16.81	0	1
289.1	3.1	6.94	10.56	14.44	16.34	1	1
290.0	4.0	7.90	8.63			0	0
291.0	5.0	8.17	9.65			0	0
292.0	6.0	9.83	11.44	17.45	20.02	0	1
293.0	7.0	10.32	12.63			0	0
294.0	8.0	11.10	13.48			0	0
295.0	10.0	10.21	12.02	17.86	19.00	0	1
296.0	11.0	10.04	11.08	16.33	20.32	0	1
297.0	12.0	8.29	13.30			1	0
298.0	13.0	7.87	9.23			0	0
299.0	14.0	6.84	9.30	12.21	16.69	0	1
299.1	14.1	6.94	8.35	12.42	15.45	0	1
300.0	15.0	7.66	8.73			0	0
300.1	15.1	7.41	8.40			0	0
301.0	16.0	7.41	10.34			0	0
301.1	16.1	6.86	10.20			1	0
302.0	18.0	8.22	9.12			0	0
302.1	18.1	7.99	8.50			0	0
303.0	19.0	7.56	8.93			0	0
303.1	19.1	7.30	10.83			1	0

TABLE C.--Raw Data from Direct (accuracy)

Tooth ID	Tooth No.	T-CEJD	T-BMD	T-FEN1D	T-FEN2D	DEHD	FEND
304.0	20.0	8.03	13.71			1	0
305.0	21.0	8.55	16.30			1	0
306.0	23.0	8.82	14.33			1	0
307.0	24.0	8.13	10.02			0	0
308.0	25.0	8.63	10.40			0	0
309.0	28.0	8.58	15.85			1	0
310.0	29.0	7.79	9.07			0	0
311.0	31.0	8.10	9.12			0	0
311.1	31.1	8.00	8.93			0	0
312.0	1.0	7.62	8.47			0	0
312.1	1.1	7.40	8.41			0	0
313.0	2.0	7.57	8.57			0	0
313.1	2.1	7.53	8.44			0	0
314.0	3.0	7.60	9.14	14.10	16.06	0	1
314.1	3.1	7.30	8.66			0	0
315.0	4.0	7.83	9.91			0	0
316.0	5.0	8.28	11.40			1	0
317.0	6.0	10.16	12.37			0	0
318.0	7.0	9.64	12.45			0	0
319.0	11.0	9.74	12.97			1	0
320.0	12.0	8.59	12.24			1	0
321.0	13.0	7.61	9.48			0	0
322.0	14.0	7.21	9.36			0	0
322.1	14.1	6.84	8.80			0	0
323.0	15.0	7.82	9.89			0	0
323.1	15.1	7.98	9.73			0	0
324.0	16.0	7.98	9.65			0	0
324.1	16.1	7.47	9.96			0	0
325.0	19.0	7.44	8.90			0	0
325.1	19.1	7.70	8.97			0	0
326.0	20.0	8.02	10.74			0	0
327.0	22.0	9.98	13.04			0	0
328.0	23.0	9.27	16.82			1	0
329.0	26.0	9.28	12.11	15.06	16.39	0	1
330.0	27.0	10.50	16.89			1	0
331.0	28.0	9.30	16.33			1	0
332.0	29.0	7.72	10.09			0	0
333.0	30.0	7.64	10.17			0	0
333.1	30.1	7.70	9.09			0	0
334.0	31.0	8.80	9.32			0	0
334.1	31.1	8.44	9.00			0	0

TABLE D.--Raw Data from CBCT (reliability)

Tooth ID	Tooth No.	t-cejc1	t-cejc2	t-bmc1	t-tbmc2	dehc1	dehc2	t-fen1c1	t-fen1c2	t-fen2c1	t-fen2c2	fenc1	fenc2	bslice1	bslice2	axial1	axial2	coron1	coron2
1.0	1.0	6.3	6.7	7.8	8.0	0	0		13.1		16.6	0	1		1		1.1		1.0
1.1	1.1	5.9	6.0	7.8	7.9	0	0	12.0	12.8	17.5	17.3	1	1	0	0	0.0	0.0	0.0	0.0
3.0	3.0	5.9	6.6	7.7	8.1	0	0	12.3	11.8	15.8	15.9	1	1	0	0	0.0	0.0	0.0	0.0
3.1	3.1	5.6	6.3	7.6	8.0	0	0	13.5	12.4	17.0	17.3	1	1	0	0	0.0	0.0	0.0	0.0
7.0	7.0	7.9	8.3	10.2	10.3	0	0		12.7		15.4	0	1		0		0.0		0.0
21.0	24.0	7.7	7.8	9.8	10.1	0	0					0	0						
34.0	7.0	10.1	10.2	12.4	12.2	0	0					0	0						
42.0	16.0	7.6	7.9	9.1	9.2	0	0		10.9		13.6	0	1		1		0.8		0.9
42.1	16.1	7.0	7.0	8.1	8.5	0	0		9.6		13.0	0	1		0		0.0		0.0
44.0	20.0	8.5	9.1	10.3	10.6	0	0					0	0						
51.0	27.0	10.9	10.6	13.3	13.4	0	0		14.5		18.9	0	1		0		0.0		0.0
63.0	10.0	9.5	9.9	12.6	12.5	1	0	16.2	15.8	19.0	18.8	1	1	0	0	0.0	0.0	0.0	0.0
71.0	19.0	6.1	6.5	7.6	7.4	0	0					0	0						
71.1	19.1	6.3	6.1	7.1	7.2	0	0					0	0						
72.0	21.0	7.5	7.7	9.4	9.9	0	0					0	0						
79.0	30.0	5.9	7.1	7.3	8.0	0	0		12.2		13.6	0	1		0		0.0		0.0
79.1	30.1	6.6	7.0	7.7	8.2	0	0		10.2		12.8	0	1		0		0.0		0.0
80.0	31.0	6.9	6.8	7.5	8.3	0	0		9.7		12.5	0	1		1		1.2		1.2
80.1	31.1	7.6	6.8	8.3	8.3	0						0							
85.0	7.0	10.8	11.3	13.7	13.9	0	0	20.4	17.8	23.7	22.8	1	1	0	0	0.0	0.0	0.0	0.0
91.0	14.0	6.9	7.5	10.8	10.9	0	0	15.7	15.9	18.0	20.8	1	1	0	0	0.0	0.0	0.0	0.0
91.1	14.1	7.0	7.2	10.6	10.8	0	0	15.5	14.9	19.5	19.3	1	1	0	0	0.0	0.0	0.0	0.0
94.0	20.0	8.9	8.6	10.9	10.3	0	0	16.8	17.1	19.1	18.7	1	1	0	0	0.0	0.0	0.0	0.0
95.0	21.0	8.8	8.5	10.9	10.8	0	0					0	0						
108.0	4.0	7.9	8.0	14.1	10.9	1	0	16.6	16.1	20.4	19.0	1	1	0	0	0.0	0.0	0.0	0.0
115.0	15.0	8.1	8.5	10.4	11.3	0	0	12.0	14.0	14.9	17.4	1	1	1	1	0.7	0.7	0.7	0.8
115.1	15.1	7.1	7.2	9.9	10.0	0	0	13.0	13.6	17.3	18.0	1	1	0	0	0.0	0.0	0.0	0.0
119.0	20.0	7.8	7.8	11.6	10.6	0	0					0							
126.0	27.0	12.0	12.0	14.1	14.1	0	0	16.2	15.5	18.4	18.2	1	1	0	0	0.0	0.0	0.0	0.0
133.0	6.0	10.3	10.4	11.6	11.9	0	0	20.1	19.1	22.6	24.3	1	1	0	0	0.0	0.0	0.0	0.0
140.0	14.0	6.5	6.7	8.5	9.5	0	0	13.1	12.5	14.7	15.3	1	1	0	0	0.0	0.0	0.0	0.0
140.1	14.0	6.9	6.9	8.6	8.9	0		11.6	13.7	16.5	17.4	1	1	0	0	0.0	0.0	0.0	0.0
145.0	21.0	7.3	7.2	11.0	8.8	1	0					0	0						
157.0	3.0	7.4	6.8	9.2	9.7	0	0	11.9	12.1	15.5	15.9	1	1	0	0	0.0	0.0	0.0	0.0
157.1	3.1	7.6	6.4	9.2	8.5	0	0	13.4	12.4	16.3	15.3	1	1	0	0	0.0	0.0	0.0	0.0
162.0	8.0	11.0	11.3	12.5	13.1	0	0	20.4	19.7	22.0	22.2	1	1	0	0	0.0	0.0	0.0	0.0
167.0	13.0	8.1	7.8	9.6	9.6	0	0					0	0						
175.0	21.0	8.4	8.1	9.2	12.7	0	1					0	0						
176.0	22.0	11.2	11.2	12.6	14.1	0	0					0	0						
179.0	25.0	9.0	9.4	10.7	11.4	0	0					0	0						
181.0	27.0	11.0	11.0	13.4	12.7	0	0		14.5		18.8	0	1		0		0.0		0.0
184.0	30.0	6.4	6.5	7.4	7.6	0	0					0	0						
184.1	30.1	6.6	6.5	7.2	7.1	0	0					0	0						
185.0	31.0	7.4	7.2	8.0	7.6	0	0					0	0						
185.1	31.1	7.6	7.1	8.1	7.8	0	0					0	0						
204.0	24.0	7.7	7.8	10.1	9.8	0	0					0	0						
209.0	29.0	6.8	6.8	9.5	9.4	0	0		11.3		14.3	0	1		0		0.0		0.0
211.0	31.0	7.3	7.9	8.6	8.4	0	0					0	0						
211.1	31.1	7.1	7.1	7.9	8.2	0	0					0	0						
212.0	2.0	6.1	6.4	8.0	8.4	0	0	12.6	13.3	15.2	15.3	1	1	1	1	1.4	1.2	1.4	1.3
212.1	2.1	6.0	6.4	8.5	8.6	0	0	11.4	13.2	15.5	15.9	1	1	1	1	1.1	1.3	1.2	1.3

TABLE D.--Raw Data from CBCT (reliability)

Tooth ID	Tooth No.	t-cejc1	t-cejc2	t-bmc1	t-tbmc2	dehc1	dehc2	t-fen1c1	t-fen1c2	t-fen2c1	t-fen2c2	fenc1	fenc2	bslice1	bslice2	axial1	axial2	coron1	coron2
215.0	8.0	12.1	12.6	15.6	15.2	1	0	19.1	18.9	25.1	24.2	1	1	1	1	1.1	1.0	1.1	1.0
216.0	9.0	12.2	12.2	14.2	14.7	0	0	16.6	16.3	20.1	18.4	1	1	1	1	0.8	0.6	0.8	0.6
217.0	10.0	11.3	11.5	13.2	12.8	0	0	16.6	14.9	20.7	17.0	1	1	0	0	0.0	0.0	0.0	0.0
221.0	15.0	7.6	7.9	8.5	8.7	0	0					0	0						
221.1	15.1	6.9	7.2	8.0	8.1	0	0					0	0						
222.0	18.0	7.6	8.0	8.8	9.1	0	0	10.1	10.2	11.7	12.0	1	1	1	1	1.4	1.0	1.4	1.2
223.0	19.0	7.6	7.5	9.0	9.0	0	0		12.5		15.8	0	1		1		0.0		0.6
223.1	19.1	7.2	7.6	9.1	9.1	0	0		11.5		15.7	0	1		1		0.7		0.9
228.0	25.0	9.9	9.6	10.9	10.6	0	0					0	0						
236.0	2.0	8.7	7.6	10.1	10.5	0	0		13.9		15.6	0	0		1		1.1		1.0
236.1	2.1	8.6	7.3	10.7	11.1	0	1	15.4	14.8	22.2	17.4	1	1	1	1	0.9	0.6	0.9	0.7
240.0	6.0	8.9	8.2	11.9	12.2	1	1					0	0						
243.0	10.0	9.4	10.1	11.9	12.5	0	0		14.8		18.9	0	1		0		0.0		0.0
246.0	15.0	8.0	8.4	10.8	10.7	0	0					0							
246.1	15.1	6.9	8.0	10.1	10.6	0	0		13.1		17.3	0	1		1		1.1		1.1
261.0	1.0	6.9	7.0	9.4	10.0	0	1	11.3		13.3		1	0	1		0.7		0.7	
261.1	1.1	6.0	6.6	9.6	10.4	0	1	10.1	11.6	14.6	14.2	1	1	1	1	0.7	0.7	0.7	0.7
266.0	8.0	12.1	10.4	14.2	12.4	0	0	16.7	19.3	21.9	23.7	1	1	0	0	0.0	0.0	0.0	0.0
274.0	19.0	6.3	6.0	8.3	8.1	0	0					0	0						
274.1	19.1	6.4	6.3	8.1	7.7	0	0					0	0						
283.0	28.0	7.5	7.3	10.9	10.7	1	1					0	0						
285.0	31.0	7.8	7.2	11.0	10.5	1	1					0	0						
285.1	31.1	7.3	7.4	8.3	8.3	0	0					0	0						
287.0	1.0	7.4	7.7	8.4	8.7	0	0	10.7	10.3	13.3	13.6	1	1	1	1	1.0	1.2	1.0	1.2
287.1	1.1	7.2	7.6	8.6	8.7	0	0	10.4	10.1	14.5	13.8	1	1	0	0	0.0	0.0	0.0	0.0
289.0	3.0	6.3	7.1	9.6	9.4	0	0	11.2	11.4	16.6	16.4	1	1	0	0	0.0	0.0	0.0	0.0
289.1	3.1	7.0	6.6	10.0	9.9	0	1	11.4	11.9	17.2	16.9	1	1	0	0	0.0	0.0	0.0	0.0
291.0	5.0	7.5	8.1	9.6	9.7	0	0	10.0	11.2	14.0	14.4	1	1	0	0	0.0	0.0	0.0	0.0
295.0	10.0	9.5	9.4	11.4	12.1	0	0		13.9		17.7	0	1		0		0.0		0.0
299.0	14.0	6.3	6.3	10.2	9.7	1	1	11.0	11.3	16.1	16.5	1	1	0	0	0.0	0.0	0.0	0.0
299.1	14.1	6.6	6.5	8.5	8.4	0	0	10.1	10.6	14.6	16.4	1	1	0	0	0.0	0.0	0.0	0.0
304.0	20.0	7.0	7.6	13.6	14.0	1	1					0	0						
309.0	28.0	8.3	8.3	14.4	13.7	1	1					0	0						
310.0	29.0	7.2	7.2	9.7	9.5	0	0	10.6	10.2	15.2	12.6	1	1	0	0	0.0	0.0	0.0	0.0
312.0	1.0	7.3	7.8	8.8	8.8	0	0	11.1	12.6	14.9	14.9	1	1	1	1	0.8	1.0	1.0	1.1
312.1	1.1	6.9	7.6	8.6	8.8	0	0	9.6	9.7	14.6	13.9	1	1	1	1	0.9	0.9	0.9	0.9
313.0	2.0	7.4	7.2	8.2	8.0	0	0		14.4		16.7	0	1		1		1.4		1.4
313.1	2.1	7.3	7.0	8.1	7.8	0	0		13.1		16.4	0	1		1		1.0		0.9
315.0	4.0	6.9	8.3	9.7	10.4	0	0	13.5	15.0	17.9	17.2	1	1	1	1	1.2	1.2	1.2	1.2
328.0	23.0	8.2	8.7	12.0	11.7	1	0	13.4	14.5	17.8	18.6	1	1	0	0	0.0	0.0	0.0	0.0

TABLE E.--Raw Data from Direct (reliability)

Tooth ID	Tooth No.	T-CEJD1	T-CEJD2	T-BM1D1	T-BM1D2	DEHD1	DEHD2	T-FEN1D1	T-FEN1D2	T-FEN2D1	T-FEN2D2	FEND1	FEND2
1.0	1.0	6.49	6.48	8.21	8.10	0	0					0	0
1.1	1.1	6.57	6.65	8.19	8.30	0	0	15.68	15.56	17.22	17.01	1	1
3.0	3.0	6.54	6.61	8.32	8.37	0	0					0	0
3.1	3.1	6.71	6.40	7.65	8.09	0	0					0	0
7.0	7.0	9.09	9.28	11.63	11.80	0	0					0	0
21.0	24.0	7.89	7.71	10.26	10.16	0	0					0	0
34.0	7.0	10.52	10.55	12.00	12.09	0	0					0	0
42.0	16.0	6.94	7.38	8.49	8.68	0	0					0	0
42.1	16.1	6.68	7.44	8.38	8.64	0	0					0	0
44.0	20.0	8.30	8.61	10.26	10.55	0	0					0	0
51.0	27.0	10.87	11.22	13.64	13.86	0	0					0	0
63.0	10.0	9.80	9.85	12.51	12.49	0	0	18.41	18.35	20.46	20.64	1	1
71.0	19.0	6.38	6.67	7.71	7.77	0	0					0	0
71.1	19.1	6.20	6.50	7.33	7.58	0	0					0	0
72.0	21.0	8.46	8.51	10.50	10.51	0	0					0	0
79.0	30.0	6.97	6.86	7.82	8.01	0	0					0	0
79.1	30.1	6.60	7.02	7.91	8.15	0	0					0	0
80.0	31.0	7.68	7.87	8.72	8.75	0	0					0	0
80.1	31.1	7.27	7.85	8.11	8.31	0	0					0	0
85.0	7.0	11.69	11.68	14.15	14.22	0	0					0	0
91.0	14.0	7.38	7.72	10.74	10.95	0	0					0	0
91.1	14.1	7.61	7.70	10.35	10.41	0	0	15.66	16.04	19.96	19.70	1	1
94.0	20.0	9.22	9.37	10.92	10.98	0	0	13.98	14.05	18.40	18.58	1	0
95.0	21.0	9.16	9.35	11.02	11.29	0	0	14.91	14.80	20.78	20.36	1	0
108.0	4.0	8.06	8.03	10.56	10.62	0	0					0	0
115.0	15.0	8.24	7.89	10.16	10.32	0	0					0	0
115.1	15.1	7.62	7.81	9.06	9.11	0	0					0	0
119.0	20.0	8.46	8.40	10.89	10.82	0	0					0	0
126.0	27.0	12.30	12.19	14.88	14.82	0	0					0	0
133.0	6.0	10.71	10.67	11.90	11.83	0	0					0	0
140.0	14.0	7.09	7.25	8.87	9.00	0	0					0	0
140.1	14.0	7.07	6.93	8.24	8.41	0	0					0	0
145.0	21.0	8.05	8.17	9.90	9.94	0	0					0	0
157.0	3.0	6.49	6.66	9.38	9.40	0	0					0	0
157.1	3.1	6.78	6.87	8.92	8.87	0	0					0	0
162.0	8.0	11.31	11.56	13.08	12.90	0	0	15.48	15.60	16.18	16.28	1	1
167.0	13.0	7.11	7.45	9.34	9.25	0	0					0	0
175.0	21.0	8.48	8.73	10.77	11.17	0	0					0	0
176.0	22.0	11.51	11.46	13.96	14.09	0	0					0	0
179.0	25.0	9.41	9.44	12.54	12.34	1	0					0	0
181.0	27.0	11.78	11.76	14.08	14.14	0	0					0	0
184.0	30.0	7.31	7.36	7.91	8.09	0	0					0	0
184.1	30.1	6.89	6.80	7.78	7.75	0	0					0	0
185.0	31.0	7.91	7.77	8.62	8.40	0	0					0	0
185.1	31.1	7.28	7.33	7.78	8.02	0	0					0	0
204.0	24.0	7.71	7.89	10.28	10.20	0	0					0	0

TABLE E.--Raw Data from Direct (reliability)

Tooth ID	Tooth No.	T-CEJD1	T-CEJD2	T-BM1D1	T-BM1D2	DEHD1	DEHD2	T-FEN1D1	T-FEN1D2	T-FEN2D1	T-FEN2D2	FEND1	FEND2
209.0	29.0	6.53	6.46	8.87	8.94	0	0					0	0
211.0	31.0	7.52	7.64	7.88	7.92	0	0					0	0
211.1	31.1	6.55	6.90	7.33	7.42	0	0					0	0
212.0	2.0	7.24	7.02	8.26	8.32	0	0					0	0
212.1	2.1	6.84	6.61	7.73	7.85	0	0					0	0
215.0	8.0	12.09	12.39	14.10	14.18	0	0					0	0
216.0	9.0	12.35	12.53	13.93	14.35	0	0					0	0
217.0	10.0	11.65	11.56	12.67	12.74	0	0					0	0
221.0	15.0	7.83	7.71	8.51	8.87	0	0					0	0
221.1	15.1	7.81	7.88	8.43	8.60	0	0					0	0
222.0	18.0	8.48	8.65	9.01	9.23	0	0					0	0
223.0	19.0	7.72	7.61	8.99	8.93	0	0					0	0
223.1	19.1	7.11	7.29	8.72	8.67	0	0					0	0
228.0	25.0	10.00	9.89	11.55	11.70	0	0					0	0
236.0	2.0	8.04	7.80	10.42	10.23	0	0					0	0
236.1	2.1	7.53	7.00	10.23	10.30	0	0					0	0
240.0	6.0	9.46	9.50	12.08	12.28	0	0					0	0
243.0	10.0	9.83	9.85	12.25	12.17	0	0					0	0
246.0	15.0	7.94	7.60	10.36	10.28	0	0					0	0
246.1	15.1	6.87	6.66	9.37	9.32	0	0					0	0
261.0	1.0	7.56	7.89	10.19	10.59	0	0					0	0
261.1	1.1	6.83	6.85	9.95	9.95	1	1					0	0
266.0	8.0	11.83	10.55	14.44	12.77	0	0					0	0
274.0	19.0	6.98	7.30	8.29	8.46	0	0					0	0
274.1	19.1	7.15	7.09	8.76	8.67	0	0					0	0
283.0	28.0	8.19	8.30	11.49	11.61	1	1					0	0
285.0	31.0	8.38	8.25	11.27	11.27	0	1					0	0
285.1	31.1	7.89	7.86	8.88	8.73	0	0					0	0
287.0	1.0	7.36	7.77	8.27	9.29	0	0					0	0
287.1	1.1	7.42	7.41	8.50	8.92	0	0					0	0
289.0	3.0	6.87	7.33	8.95	8.88	0	0	12.91	12.83	16.81	16.95	1	1
289.1	3.1	6.94	7.26	10.56	10.85	1	1	14.44	13.97	16.34	16.56	1	1
291.0	5.0	8.17	8.17	9.65	9.70	0	0					0	0
295.0	10.0	10.21	10.35	12.02	12.49	0	0	17.86	17.82	19.00	19.16	1	1
299.0	14.0	6.84	7.06	9.30	9.37	0	0	12.21	11.82	16.69	16.75	1	1
299.1	14.1	6.94	7.25	8.35	8.56	0	0	12.42	12.02	15.45	15.57	1	1
304.0	20.0	8.03	8.06	13.71	13.80	1	1					0	0
309.0	28.0	8.58	8.59	15.85	15.85	1	1					0	0
310.0	29.0	7.79	7.85	9.07	9.26	0	0					0	0
312.0	1.0	7.62	7.95	8.47	8.98	0	0					0	0
312.1	1.1	7.40	7.53	8.41	8.62	0	0					0	0
313.0	2.0	7.57	7.78	8.57	8.87	0	0					0	0
313.1	2.1	7.53	7.73	8.44	8.94	0	0					0	0
315.0	4.0	7.83	7.99	9.91	9.92	0						0	
328.0	23.0	9.27	9.30	16.82	16.84	1	1					0	0

REFERENCES

Aboudara CA, Hatcher D, Nielsen IL, Miller A. A three-dimensional evaluation of the upper airway in adolescents. Orthod Craniofac Res. 2003;6 Suppl 1:173-5.

Cevidanes LH, Styner MA, Proffit WR. Image analysis and superimposition of 3-dimensional cone-beam computed tomography models. Am J Orthod Dentofacial Orthop. 2006 May;129(5):611-8.

Cevidanes LH, Bailey LJ, Tucker SF, Styner MA, Mol A, Phillips CL, Proffit WR, Turvey T. Three-dimensional cone-beam computed tomography for assessment of mandibular changes after orthognathic surgery. Am J Orthod Dentofacial Orthop. 2007 Jan;131(1):44-50.

Garg AK. Dental implant imaging: TeraRecon's Dental 3D Cone Beam Computed Tomography System. Dent Implantol Update. 2007 Jun;18(6):41-5.

Hatcher DC, Dial C, Mayorga C. Cone beam CT for pre-surgical assessment of implant sites. J Calif Dent Assoc. 2003 Nov;31(11):825-33.

Hatcher DC, Aboudara CL. Diagnosis goes digital. Am J Orthod Dentofacial Orthop. 2004 Apr;125(4):512-5.

Hilgers ML, Scarfe WC, Scheetz JP, Farman AG. Accuracy of linear temporomandibular joint measurements with cone beam computed tomography and digital cephalometric radiography. Am J Orthod Dentofacial Orthop. 2005 Dec;128(6):803-11.

Hintze H, Wiese M, Wenzel A. Cone beam CT and conventional tomography for the detection of morphological temporomandibular joint changes. Dentomaxillofac Radiol. 2007 May;36(4):192-7.

Hoffman EA, Sinak LJ, Robb RA, Ritman EL. Noninvasive quantitative imaging of shape and volume of lungs. J Appl Physiol. 1983 May;54(5):1414-21.

Honda K, Arai Y, Kashima M, Takano Y, Sawada K, Ejima K, Iwai K. Evaluation of the usefulness of the limited cone-

beam CT (3DX) in the assessment of the thickness of the roof of the glenoid fossa of the temporomandibular joint. Dentomaxillofac Radiol. 2004 Nov;33(6):391-5.

Honda K, Matumoto K, Kashima M, Takano Y, Kawashima S, Arai Y. Single air contrast arthrography for temporomandibular joint disorder using limited cone beam computed tomography for dental use. Dentomaxillofac Radiol. 2004 Jul;33(4):271-3.

Honda K, Bjornland T. Image-guided puncture technique for the superior temporomandibular joint space: value of cone beam computed tomography (CBCT). Oral Surg Oral Med Oral Pathol Oral Radiol Endod. 2006 Sep;102(3):281-6.

Iwasaki T, Ritman EL, Fiksen-Olsen MJ, Romero JC, Knox FG. Renal cortical perfusion--preliminary experience with the dynamic spatial reconstructor (DSR). Ann Biomed Eng. 1985;13(3-4):259-71.

Kobayashi K, Shimoda S, Nakagawa Y, Yamamoto A. Accuracy in measurement of distance using limited cone-beam computerized tomography. Int J Oral Maxillofac Implants. 2004 Mar-Apr;19(2):228-31.

Lascala CA, Panella J, Marques MM. Analysis of the accuracy of linear measurements obtained by cone beam computed tomography (CBCT-NewTom). Dentomaxillofac Radiol. 2004 Sep;33(5):291-4.

Liu DG, Zhang WL, Zhang ZY, Wu YT, Ma XC. Localization of impacted maxillary canines and observation of adjacent incisor resorption with cone-beam computed tomography. Oral Surg Oral Med Oral Pathol Oral Radiol Endod. 2008 Jan;105(1):91-8.

Loubele M, Maes F, Schutyser F, Marchal G, Jacobs R, Suetens P. Assessment of bone segmentation quality of cone-beam CT versus multislice spiral CT: a pilot study. Oral Surg Oral Med Oral Pathol Oral Radiol Endod. 2006 Aug;102(2):225-34.

Maes F, Collignon A, Vandermeulen D, Marchal G, Suetens P. Multimodality image registration by maximization of

mutual information. IEEE Trans Med Imaging. 1997 Apr;16(2):187-98.

Maki K, Inou N, Takanishi A, Miller AJ. Computer-assisted simulations in orthodontic diagnosis and the application of a new cone beam X-ray computed tomography. Orthod Craniofac Res. 2003;6 Suppl 1:95-101; discussion 79-82.

Marmulla R, Wortche R, Muhling J, Hassfeld S. Geometric accuracy of the NewTom 9000 Cone Beam CT. Dentomaxillofac Radiol. 2005 Jan;34(1):28-31.

Mengel R, Candir M, Shiratori K, Flores-de-Jacoby L. Digital volume tomography in the diagnosis of periodontal defects: an in vitro study on native pig and human mandibles. J Periodontol. 2005 May;76(5):665-73.

Nakagawa Y, Kobayashi K, Ishii H, Mishima A, Asada K, Ishibashi K. Preoperative application of limited cone beam computerized tomography as an assessment tool before minor oral surgery. Int J Oral Maxillofac Surg. 2002 Jun;31(3):322-6.

Nakajima A, Sameshima GT, Arai Y, Homme Y, Shimizu N, Dougherty H, Sr. Two- and three-dimensional orthodontic imaging using limited cone beam-computed tomography. Angle Orthod. 2005 Nov;75(6):895-903.

Ogawa T, Enciso R, Memon A, Mah JK, Clark GT. Evaluation of 3D airway imaging of obstructive sleep apnea with cone-beam computed tomography. Stud Health Technol Inform. 2005;111:365-8.

Pawelzik J, Cohnen M, Willers R, Becker J. A comparison of conventional panoramic radiographs with volumetric computed tomography images in the preoperative assessment of impacted mandibular third molars. J Oral Maxillofac Surg. 2002 Sep;60(9):979-84.

Pinsky HM, Dyda S, Pinsky RW, Misch KA, Sarment DP. Accuracy of three-dimensional measurements using cone-beam CT. Dentomaxillofac Radiol. 2006 Nov;35(6):410-6.

Ritman EL, Kinsey JH, Robb RA, Gilbert BK, Harris LD, Wood EH. Three-dimensional imaging of heart, lungs, and circulation. Science. 1980 Oct 17;210(4467):273-80.

Sato S, Arai Y, Shinoda K, Ito K. Clinical application of a new cone-beam computerized tomography system to assess multiple two-dimensional images for the preoperative treatment planning of maxillary implants: case reports. Quintessence Int. 2004 Jul-Aug;35(7):525-8.

Scarfe WC, Farman AG, Sukovic P. Clinical applications of cone-beam computed tomography in dental practice. J Can Dent Assoc. 2006 Feb;72(1):75-80.

Schulze D, Blessmann M, Pohlenz P, Wagner KW, Heiland M. Diagnostic criteria for the detection of mandibular osteomyelitis using cone-beam computed tomography. Dentomaxillofac Radiol. 2006 Jul;35(4):232-5.

Tsiklakis K, Syriopoulos K, Stamatakis HC. Radiographic examination of the temporomandibular joint using cone beam computed tomography. Dentomaxillofac Radiol. 2004 May;33(3):196-201.

Walker L, Enciso R, Mah J. Three-dimensional localization of maxillary canines with cone-beam computed tomography. Am J Orthod Dentofacial Orthop. 2005 Oct;128(4):418-23.

79 279 CW 5830
TH
08/08 00-104-07 Ohio

